ABSTRACT

VARIATION IN EXOPLANETARY STRUCTURE
AND MINERALOGY FROM OBSERVED
STELLAR METALLICITIES, AND
RELATED GEOPHYSICAL
IMPLICATIONS

Despite the detection of thousands of exoplanetary candidates, too few of these are known to resemble Earth in terms of volume and composition for many meaningful statistics on Earth-sized exoplanets to be obtained. Therefore, we instead estimate the bulk mineralogy of Earth-sized planet models, using the emission spectra of Sun-like stars. It is possible to convert the results of many stellar spectral observations into major oxides, thus allowing conversion of these oxides to silicate mantle mineralogies, similar to work done by Unterborn et al. (2017), as well as estimate the relative volume of a metallic core for cases where terrestrial worlds are near Earth's size. This approach provides a way to anticipate how such exoplanets may differ from Earth structurally, compositionally, and perhaps in terms of geologic behavior. In order to isolate the effects on an otherwise Earth-analogue planet due only to initial variations in elemental composition, the volume, surface temperature, hydrosphere, and atmosphere are all considered equal to Earth, as differences in these aspects of a planet are not directly linked to the composition of the host star. The goal is to increase understanding of effects due solely to differences in initial bulk chemical composition and provide improved mineralogical and geophysical constraints of planets which may orbit roughly solar-analogue stars.

John Carleton Rarick
May 2018

VARIATION IN EXOPLANETARY STRUCTURE AND MINERALOGY FROM OBSERVED STELLAR METALLICITIES, AND RELATED GEOPHYSICAL IMPLICATIONS

by

John Carleton Rarick

A thesis

submitted in partial

fulfillment of the requirements for the degree of

Master of Science in Geology

in the College of Science and Mathematics

California State University, Fresno

May 2018

APPROVED

For the Department of Geology:

We, the undersigned, certify that the thesis of the following student meets the required standards of scholarship, format, and style of the university and the student's graduate degree program for the awarding of the master's degree.

John Carleton Rarick
Thesis Author

Keith Putirka (Chair) Geology

Alain Plattner Geology

John Wakabayashi Geology

For the University Graduate Committee:

Dean, Division of Graduate Studies

AUTHORIZATION FOR REPRODUCTION

OF MASTER'S THESIS

_____ I grant permission for the reproduction of this thesis in part or in its entirety without further authorization from me, on the condition that the person or agency requesting reproduction absorbs the cost and provides proper acknowledgment of authorship.

__X__ Permission to reproduce this thesis in part or in its entirety must be obtained from me.

Signature of thesis author:_____

ACKNOWLEDGMENTS

Academically, I would like to graciously thank Dr. Keith D. Putirka for his constant guidance, support of, and enjoyment taken in my overall academic success, and specifically in this thesis. Dr. John Wakabayashi and Dr. Alain Plattner for their expertise, valuable contributions to, and review of this study, and Dr. Ronald Rarick for additional constructive reviews of the manuscript.

Generally, I would like to thank my parents, Lucinda Jane Friend Rarick and Ronald Dale Rarick for their unfailing love, and support of my endeavors even when those seem strange. Additionally, I would like to thank the Putirka family for their trust and friendship above and beyond expectations.

Finally, I would like to thank Wendy Cooper for her efforts on my behalf to secure for me a part-time staff position with the Department of Biology, without which the completion of this thesis would have required considerably more time and expense.

TABLE OF CONTENTS

Page

LIST OF TABLES

Page

LIST OF FIGURES

Page

Page

INTRODUCTION

The Solar Nebula Disk Model (SNDM) states that the Sun and all other natural objects in orbit were formed together from the same gravitationally compressed, flattened, and rotating disk of interstellar gas and dust (Swedenborg 1734; Laplace 1796; Safronov 1972). This process of formation is thought to be the same for all other known main-sequence stars and their planetary systems (Coradini 1981; Bradford & Terrile 1984). In accordance with SNDM, the terrestrial planets of the Solar System, including Earth, share a bulk elemental composition very like that of the Sun for non-gaseous elements (Wood 1979). This close correlation may be demonstrated by comparing the elemental abundances observed in the Sun's emission spectrum with those found in carbonaceous chondritic meteorites (Figure 1), the same kind of meteorites hypothesized to have formed Earth (Pottasch 1964; Ringwood 1966; Lodders et al; 2003).

These meteorites are undifferentiated objects thought to originate from before the formation of the planets, and thus preserve, in solid form, elements in the precise relative abundances found in the proto-stellar disk from which the Sun and planets formed (McSween 1979; McKeegan et al, 2011).

It has been observed that the relative elemental abundances in the emission spectra from our Sun's photosphere closely match Earth's bulk composition, and by implication, observations of the emission spectra of other stars may allow for the determination of bulk elemental compositions of any exoplanet-masses that may have formed around those stars (Lineweaver & Robles 2009; Hinkel et al, 2014). If data on enough spectra are obtained, it may become possible to assemble a comprehensive dataset of the range of possible terrestrial exoplanetary bulk compositions. In this approach, it is assumed that exoplanetary volumes are

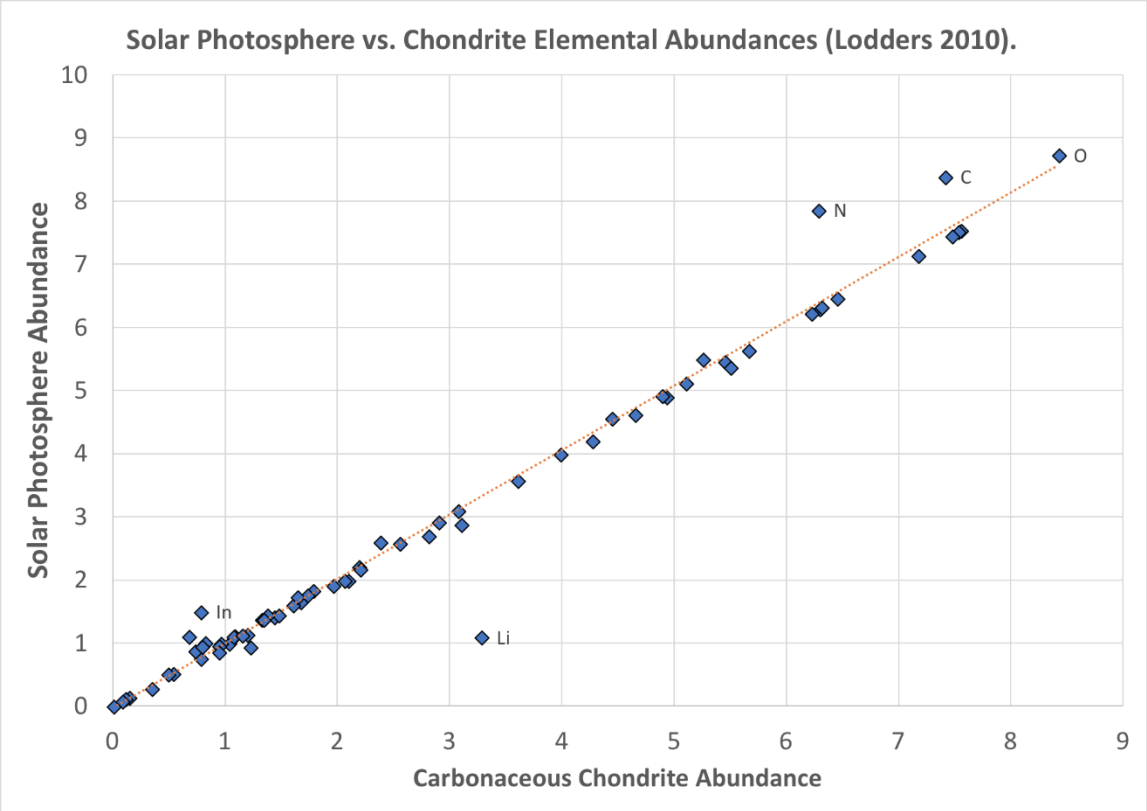

Figure 1. Demonstration of strong correlation between elemental abundances of the solar photosphere and carbonaceous chondritic meteorites.

Note: Li is depleted in the solar atmosphere due to its conversion to He during nuclear fusion. C, N, and O are slightly enhanced due to a small but non-trivial amount of solar energy output produced by the C-N-O cycle catalytic fusion process.

similar to Earth for the sake of making more direct comparisons. This is because if planetary size changes to any substantial degree, the result will be planets that do not resemble Earth in any way no matter what their elemental composition. From our exoplanet bulk composition estimates, we can use total Fe contents, and Earth's relative core and mantle compositions, to infer the total mass of an exoplanet's metallic core, allowing all other oxides to form a silicate mantle and crust, which we call the Bulk Silicate Planet (BSP) composition. The BSP oxides may then be used to determine mineralogy of an exoplanet's silicate mantle. After such a determination, hypotheses may be formulated regarding the nature of planetary-scale geologic processes occurring on the worlds in question. One such hypothesis is that the mineralogy of a mantle should affect mantle circulation and the operation of plate tectonics. The exact magnitude of these effects remains quite uncertain to be sure, but we still propose to offer some speculation, given advances in modeling mantle and subduction processes.

There have been several groups that have attempted studies of potential planetary compositions (i.e. Jura et al. 2014; Marcy et al. 2014; Zeng et al. 2016). However, they are generally conducted more from an astrophysical perspective, than a mineralogical one. It is a matter of concern that their focus is on only a few or even a single element ratio, typically Fe/H, Mg/H, or Mg/Si (e.g. Sotin et al, 2007; Mena et al, 2010). While serving as an intriguing start to the problem of exoplanet composition, the numbers of elements are too few to place constraints on mantle mineralogy. For example, it is impossible to place such constraints on clinopyroxene (Cpx) abundances without CaO, nor garnet compositions in the absence of Al_2O_3, and both these minerals are essential components of Earth's upper mantle as a whole (e.g. Frost 2008; Kaminsky 2012). We thus need to discern at least the relative abundances of Si, Al, Fe, Mg, and Ca even to begin to

portray in some reasonable fashion an exoplanet's mineralogy. In addition, many studies (e.g. O'Neill & Lenardic 2007, Valencia & O'Connell 2009) on various planetary characteristics often focus on a small collection of already observed exoplanets, all of which are more massive than Earth. Hence their geologic processes are more speculative than estimations based on Earth-sized planets due to the potential influence of higher bulk density, gravity, and massive hydrospheres and/or atmospheres (Dressing et al, 2015). There is also a range of studies performed on the compositions of exoplanetary candidates observed by the Kepler Space Telescope (KST). However, the extent to which the characteristics of these candidate planets correlate to the planetary models described in this study are limited due to the biases inherent in the observational nature of the initial Kepler mission, and even more so for detected planets of the K2 mission, which is limited to observations lasting 80 days at a time, thus reducing the probability of detecting planets in longer period orbits, regardless of the type of star being orbited (Vanderburg et al, 2016). Specifically, the Kepler-derived data are biased towards larger planets in close orbits of stars similar in luminosity to the Sun (Borucki et al, 2011; Howard et al. 2012, Batalha et al. 2013; Morton & Johnson 2011). As the models developed for this study require the planet's mass be held at a constant of $1M_{\oplus}$, most Kepler mission candidate planets fall outside the parameter space in which the models of this study operate. Because this study does not rely on previously detected planetary candidates but only on stellar spectra, a wider range of potential exoplanet compositions may be explored, including a number that may be similar enough to Earth to mimic its mineralogical features.

It may also be possible to isolate some impact on tectonics specific to changes in minerology by holding constant previously stated factors.

Data and General Approach

All stellar spectra used in this study are taken from the Hypatia Catalog (HC) (Hinkel et al, 2014). For many of these stars only one to three elements are reported, fewer than the nine major oxides that influence the bulk mineralogy and bulk properties of Earth, these being; SiO_2, TiO_2, Cr_2O_3, Al_2O_3, FeO, MgO, NiO, CaO, Na_2O. We find that of the 3,058 listed stars, 893 provide the required number of heavy element/H ratios to delineate a useful mineral assemblage.

As defined by the Morgan-Keenan (MK) classification system (Morgan et al. 1943), 105 (11.8 %) of these 893 selected stars fall within the K class interval as defined by the MK system, with these stars varying between the K5 and K0 subclasses. 437 (48.9 %) cover the entire G class range from G9 to G0, and 351 (39.3 %) include F9 through F2 within the F class sequence. The statistical distribution of the number of stars representing each stellar class in this study is such that the Sun, an MK G2V class main-sequence star, falls very close to the mean of the stars chosen for this study in terms of mass and luminosity.

To understand where the Sun plots relative to other stars in terms of its composition of elements heavier than H and He, i.e. its “metallicity”, is critical. The HC, Hinkel et al. (2014) uses the solar metallicity value of 0.0141 reported by Lodders et al. (2009), as the baseline for all other stars in the catalogue to be compared against. As this study is based on the HC, it will utilize the same baseline 0.0141 metallicity value for the Sun as the HC.

Fe and Ni proportions are used to determine the mass of a planetary core relative to the total planet mass as we see similar partitioning between Earth and Venus. However, this partitioning may vary under O-saturated or O-depleted conditions (Taylor 2013). Using Earth as a presumed archetype, the extent of mantle Fe depletion in Earth’s mantle (relative to a chondritic bulk composition)

was determined, and then applied to our model planets. With a mantle so depleted in Fe and Ni, the remaining Fe, converted to FeO, and other oxides are then transformed into mineral proportions using the algebraic method of-Thompson (1982), a process explained in greater detail in the Methods section. Since the size of the core is slightly different for each model exoplanet, even if we fix the planetary radius to be the same as Earth, we must re-calculate gravity as a function of depth for each exoplanet. Pressure is-calculated as a function of depth using these new gravity values, and P-sensitive mineral phase transformations, e.g. Ol to spinel; spinel to perovskite, etc. (Stixrude & Bertelloni 2011).

BACKGROUND

The photosphere of the Sun, or any other main-sequence star of similar mass, is a comparatively thin layer, approximately 100-200 km deep, composed of cool plasma at 5800 K (Solanki 1998). This temperature varies depending on the class of the star in question. The photosphere is the lowest layer of the solar atmosphere and is the uppermost region of the Sun where, moving outward, the plasma density becomes low enough for the free transmission and absorption of photons (Grevesse & Sauval 1998). Therefore, this layer represents the Sun's "surface", i.e. what is seen when looking at the Sun directly (Solanki 1998).

When a spectrum is obtained from visible sunlight, which passes through the photosphere, parallel dark lines of varying thickness will appear across the spectrum when it is laid out as a 1-D plot. These absorption lines form due to the presence of specific elements in the tenuous plasma of the solar photosphere where each element, due to its unique electron orbitals will absorb photons at a specific wavelength thus producing a dark band across a specific section of the spectrum (Walsh 1955). The width of these absorption lines correspond to the relative abundance of the element absorbing that specific wavelength of light, whereas the line placement along the spectrum represent specific elements, as each element will create its own absorption line in the same place, regardless of the star. (Herschel 1823; Kirchhoff & Bunsen 1860; Minnaert 1930; Unsöld & Struve, 1940). The elemental composition of a star's photosphere is thought to be a reliable indicator of that star's bulk composition (Grevesse & Sauval 1998). Therefore, the absorption lines in the emission spectra from the Sun, or another main-sequence star, may be used to determine the relative ratio of elemental abundances composing that star (Payne 1925; Russell et al. 1935).

When the Sun formed in the center of its proto-stellar disk at 4.57 Ga, (Bonanno et al. 2002; Connelly et al. 2012) the process of gravitational collapse did not completely incorporate all the material of the disk into the Sun (Safronov 1972). This leftover disk material was further reduced by the effects of solar radiation and gravitational ejection of forming planetary bodies, such that only 0.14% of the mass of the solar nebula remained to be incorporated into all the planets and other objects in orbit of the Sun today (Safronov 1972; Wood 1979; McSween 1979; Woolfson 2000).

The first objects to coalesce out of the proto-planetary disk were too low in mass, and contained too little internal heat, to allow for Fe, Ni, and other siderophile elements, elements which readily dissolve into solution with Fe, to precipitate out of solution and thus become differentiated bodies with layers of siderophile element depletion (Davis 2006; Elser et al. 2012). Though most of these early objects were later incorporated into larger, differentiated bodies, some presently remain in the solar system. These are referred to as chondrites, named for the prevalence of spherical, glassy, often carbon-rich chondrules found throughout the bodies of these meteorites (Shu et al. 1996, Jones et al 2000). As these chondrite meteorites formed directly from the same material as the Sun, they possess an elemental composition that more closely matches the Sun than any other single material to be found in the present Solar System (Wood 1979; McDonough and Sun 1995; McDonough 2000; Wade and Wood 2005).

Even as the Sun formed, dust from the solar nebula aggregated into primitive material that formed planetesimals/asteroids (Poppe et al. 2000; Marshall & Cuzzi 2001), which then accreted into protoplanets with masses between roughly 0.1% and 10% the mass of Earth (Chambers 2004). These in turn collided with each other, resulting in the formation of planets. When the frequency and

kinetic energy of such collisions becomes sufficient, these accreting bodies will be enveloped by a magma ocean, which as they solidify, may later be periodically re-formed by occasional increased rates of surface bombardment, or single massive impacts. (Wood 1979; Warren 1985; Tonks & Melosh 1993).

As the growing planet gains mass, its increased internal temperature and gravity become ever more capable of segregating elements based on phase. (Jones & Drake 1986; Gaetani & Grove 1997). Iron and other siderophile elements precipitate out of solution, and once formed, these metallic pockets, being denser than the surrounding silicates, begin to sink towards the center of the protoplanet, forming a metallic core (Stevenson et al. 1983; Jones & Drake 1986; Chambers 2004; Wade & Wood 2005; Yanick et al. 2009; Rubie et al. 2011). Earth's core was formed progressively, throughout the major accretionary period, such that it was already in place at the end of planetary accretion (Anderson 2007). The residual silicate mantle is thus depleted in the elements that segregated to form the core (Halliday 2004; Davies 2006; Yanick et al. 2009; Rubie et al. 2011). Later, on Earth at least, the crust, oceanic and then continental, was extracted from partial melting of the mantle (Hoffman 1988). Earth's bulk composition would, of course, be a weighted average of Earth's core, mantle, crust, oceans and atmosphere, and should, in theory, closely resemble the chondrites (Figure 2), of which Earth is, presumably, composed (Russell 1941; Ringwood 1975; Smith 1977; Wood 1979; Hart 1986; McDonough & Sun 1995; Drake 2002).

Presently there is no known type of meteorite whose composition matches current estimates of Earth's bulk composition, though these estimates themselves may be in error. Carbonaceous chondrites (C-chondrites), defined by relatively high concentrations of organic matter, including amino acids (Ehrenfreund et al. 2001) represent one group, and Enstatite chondrites (E-chondrites), a form of very

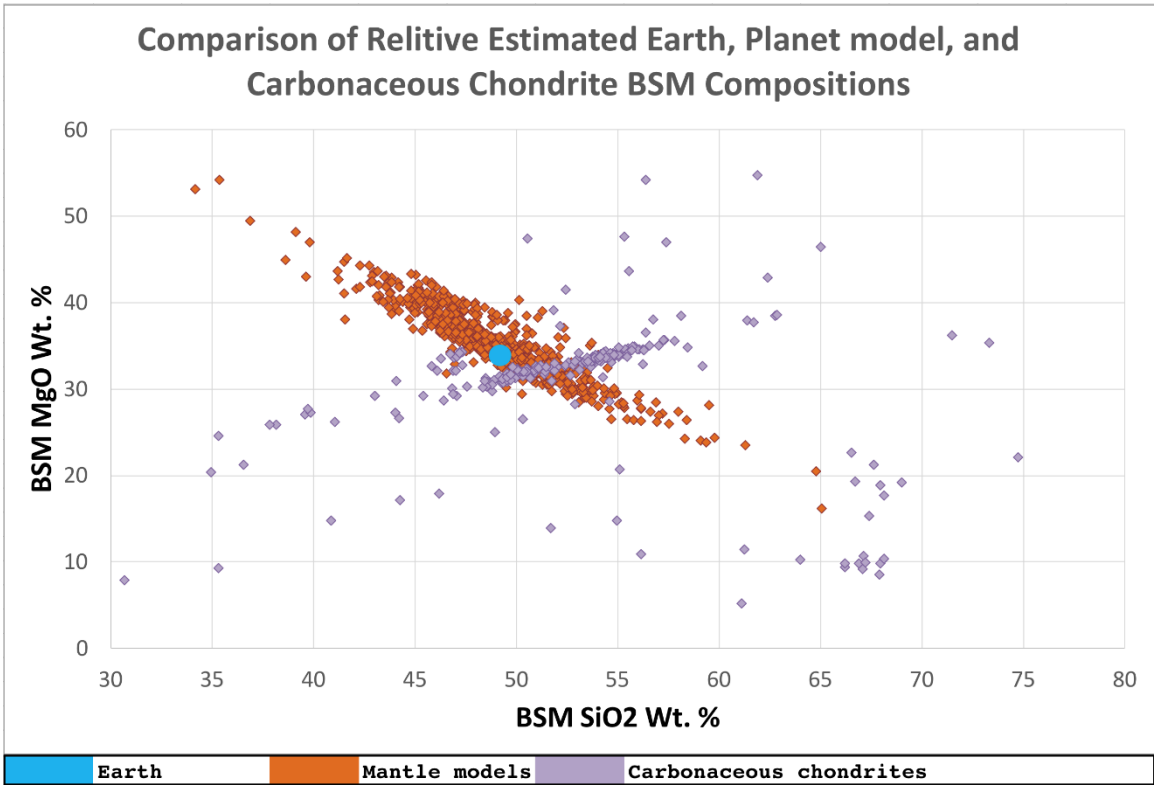

Figure 2. Composition of a theoretical "Bulk Silicate Mantle" (BSM) for various chondrite types compared with our model exoplanet mantles and the Earth's BSM. *Note*: The Earth does not precisely match any of the highly variable chondrite compositions.

O-poor chondrite, another. Early research suggests that C-chondrites could represent much of the material from which the Earth was formed, though they failed to account for the comparatively high terrestrial O^{18} abundances representative of the bulk Earth composition (Clayton 1977; McDonough & Sun 1995). However, E-chondrites display O isotope ratios much closer to the Bulk Silicate Earth (BSE) (Javoy et al. 2010). It was considered for a while that E-chondrites might represent the true building blocks of Earth. However, problems became apparent when studies showed that E-chondrites could not account for compositional dissimilarities in Si isotope ratios as compared to the Earth and the Moon as these two bodies share nearly identical Si isotope ratios of around $\delta^{30}Si_{BSE} = -0.28$, Where E-chondrites fall closer to $\delta^{30}Si_{BSE} = -0.62$, implying that

the Earth gained its current compositional ratios post moon-forming impact (Fitoussi et al. 2012). In addition, Sm/Nd isotope ratios as compared to the BSE, are 4.5-7.9% higher for the BSE as compared to chondrites. (Jackson & Jellinek 2013).

More recent studies reveal that Mo, Nd, and Sm isotopic ratios point to Earth having largely formed from s-process (slow neutron capture) material (Render et al. 2017). The composition of this material is believed to be derived from nucleosynthetic enrichment of elements heavier than Fe in asymptotic giant branch (AGB) stars (Burbidge et al. 1957). No meteoritic sample of this material has yet been identified and so cannot be compared directly to Earth's composition (Render et al. 2017). Current understanding of Earth's true composition, while good, may not be sufficient to determine affinity with any one meteorite type, chondritic or otherwise. Regardless, since there is no *a priori* reason why Earth must be composed of any one type of meteorite, the possibility that Earth is composed of a mixture of materials is strong.

Earth has changed little in terms of bulk composition since the Moon-forming impact at 4.5 Ga (Canup & Asphaug 2001), and the presumed late-veneer additions to the mantle (Kruijer et al. 2015; Fischer-Gödde et al. 2017). We reproduce estimates by Anderson & Kovach 1967, and Morgan & Anders 1980, that the Earth's Iron-Nickel core comprises approximately 32% of the total planetary mass, and 16% of its volume, while the silicate mantle accounts for 67% of the Earth's mass and 82% of its volume. The remaining mass and volume are accounted for by the Earth's crust, hydrosphere, and atmosphere.

Various seismological studies and numerical models have identified a series of discontinuous layers in the mantle structure (Mohorovičić 1909; Ringwood 1962; Clarke & Ringwood 1964; Isacks et al. 1968; Woodhouse &

Dziewonski 1984). The depth and cause of these discontinuities is generally agreed upon, with minor variations in interpretation. The region extending down from the Mohorovičić discontinuity (Moho) (beginning at an average depth of 35 km for continental crust, and 7 km for oceanic crust) to a depth of 440 km is the uppermost part of the mantle. For Earth, this layer is peridotite (Mohorovičić 1909; Helffrich and Wood 2001; Frost 2008). At a depth of around 200 km, down to 400-450 km, with pressures beginning at around 8 GPa and increasing to 17 GPa, the mineralogy is characterized by garnet-peridotite (Stixrude & Lithgow-Bertelloni 2011). Beneath the continents, there is a seismic discontinuity known as the Lehmann discontinuity (Lehmann 1959; Hales et al. 1980; Karato 1992), which occurs at around 220 km in depth and is thought to represent depth variation in shear wave anisotropy (Savage et al. 2004).

Beginning around 410 km, and continuing to roughly 520 km, a new seismic regime exists, created by the transition of olivine to β-phase spinel, called wadsleyite, and then from 550-670 km this phase converts to γ-phase or Ringwoodite (Ringwood 1968; Smith 1983; Kudoh et al. 1996). This interval from 440 to 670 km is called the Transition Zone (Inoue et al. 1998; Anderson 2007; Yoshino 2008; Pearson et al. 2014). Earth's lower mantle extends from 670 km to the core-mantle boundary at a depth of 2,891 km (Dziewonski & Anderson 1981; Hama & Suito 2001), where ferrosilicate perovskite and magnesiowüstite (transformation products of transition zone minerals) dominate the mineralogy of Earth's lower mantle (Frost et al. 2004).

The specific effects on planetary dynamics due to changes in core size and mantle thickness or composition is the subject of some debate (Unterborn et al. 2017). One potential difference might be a correlation between increased mass, and thus surface gravity, leading to more favorable conditions for a basalt to

eclogite phase transition in crustal material, a transformation unusual on Earth outside of subduction zones (O'Rourke & Korenaga 2012). Another such example is that increases in Si and the alkali elements Na and K might result in more buoyant crust being formed, reducing the effectiveness of subduction relative to Earth's crust, thereby delaying or preventing the onset of plate tectonics (Unterborn et al. 2017). The opposite effect may result when abundances of Si, Na, and K, which are incompatible in planetary melting processes, are reduced, leading to a denser crust that may subduct more easily (Unterborn et al. 2017). These examples demonstrate that an Earth-sized planet's ability to develop plate tectonics may also be influenced by the chemical composition of its mantle and crust in addition to the influences of mass, surface gravity, internal and surface temperature, and radiogenic element concentration.

Perhaps one of the most critical components in determining the existence of plate tectonics is the presence or lack of surface water (Korenaga 2010; Hull et al. 2016). The prevailing theory that the crust of Venus is too dry to produce Earth-like plate motion, resulting is episodic planet wide resurfacing events every 200-500Ma, would seem to provide strong support to this hypothesis. (e.g. Phillips et al. 1992; Smrekar & Davaille 2016). Therefore, it is quite possible that as this study concerns itself only with changes in planetary bulk material properties, it lacks the ability to predict any specific tectonic regime.

In all, as terrestrial planets in orbit of main-sequence dwarf stars are quite common (e.g. Morton & Johnson 2011; Batalha et al. 2013; Petigura et al. 2013), the potential exists for a wide range of possible tectonic scenarios.

METHODS

For this study, all required stellar spectra observations are from the Hypatia Catalogue (Hinkle et al. 2014). This catalog contains 3,058 F, G, and K main-sequence stars that cover a range of energies, from K5V orange dwarfs (least energetic), to a F2 white main-sequence star (the most energetic). This specific range in stellar classes is of fundamental importance as those stars which fall beyond it have characteristics that likely prevent them from hosting planets which could achieve an Earth-like tectonic regime, regardless of composition, at least for extended periods (Figure 3). For instance, stars with masses below about 50% that of the Sun are ignored as they have sufficiently low luminosities that for a planet like the Earth to receive the necessary incident IR flux per unit of surface area to experience sufficient heating to preserve liquid surface water, an orbital radius of 0.4 AU or less is required.

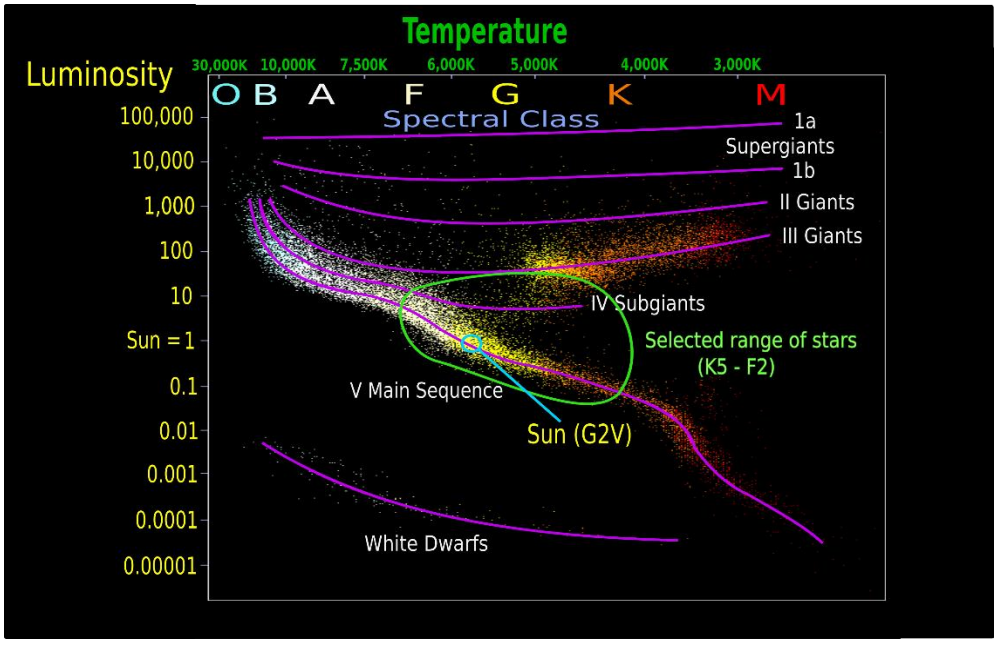

Figure 3. Hertzsprung-Russel (HR) diagram showing placement of 22,000 stars from the Hipparcos catalogue and a further 1,000 from the Gliese catalogue.
Note: "Selected range of stars" region covers the variety of stars listed in the Hypatia Catalogue. The Sun as a G2V class main-sequence star occupies a position in the mid-upper G class range, as denoted by the blue circle.

These close orbits make such planets particularly vulnerable to the characteristic frequent Coronal Mass Ejections (CMEs) of low luminosity stars (Khodachenko et al. 2007; Segura et al. 2010; Opher & Kornbleuth 2016). This proximity may cause oceanic and atmospheric ablation by charged particles resulting in the loss of both hydrosphere and atmosphere. These CMEs may increase the star's luminosity by a factor of 100 or more for a period of several hours and output an equal increase of UV and X-ray radiation (Lovell 1971; Engle & Guinan 2011). Therefore, for such stars the possibility of an Earth-sized planet with a hydrosphere similar to Earth's cannot be safely assumed.

As for stars with luminosities beyond the most powerful stars in this study (>1.3 Solar masses), these are ignored because their nucleosynthetic processes are dominated by the Carbon-Nitrogen-Oxygen (CNO) cycle (Weizsäcker 1938; Bethe 1939), a highly temperature sensitive catalytic process which only becomes dominant at temperatures above 17 megakelvin—higher than the Sun's core temperature of 15.7 megakelvin (Schuler & King 2009). Thus, the core regions of stars only slightly more massive than the Sun transition to a mostly convective state, as opposed to our Sun's dominantly conductive core. This allows for a greater percentage of the star's H to be mixed with the He fusion products, shortening their main-sequence life (Moore & Garaud 2016) such that they transition off the main sequence to a red giant stage within only a few hundred Ma. (Iben 1967; Goldstein 1987). This event therefore, would preclude the initiation of Earth-like plate tectonic motion (e.g. O'Neill 2007; Condie 2008).

The 3,058 listed stars in the HC were filtered to obtain a subset of 893 stars where all the following element ratios are reported: Al/H, Ca/H, Cr/H, Fe/H, Mg/H, Na/H, Ni/H, Si/H, Ti/H. These ratios were reported in the decimal exponent (dex) format, where the ratio is applied as an exponent to a base 10, and the value is relative to the Sun. Therefore, if log [Al/H] = 0.08, then the atomic

ratio Al/H = $10^{0.08}$, which indicates that the Al/H ratio of the star in question is $10^{0.08}$ = 1.202 times the Al/H value for the Sun. In many cases, multiple ratios from several separate sources per star, as listed in the HC, were provided for the same elements; in these cases, the dex values are averaged.

These element ratios were converted to oxide percent values: NiO, FeO, Cr_2O_3, TiO_2 CaO, SiO_2, Al_2O_3, MgO, Na_2O using a conversion procedure provided by Hinkle et al. (2014). This procedure begins by employing estimates of atomic abundances of the solar photosphere relative to H, provided by Lodders et al. (2003). These values range from 83176.4 [Ti/H] to 3.5x10^7 [Si/H]. The reported abundance value for each element "El" is calculated in the form A(El)^{10},

where:

$$A(El) = log \in (El) = \log\left[\frac{n(El)}{n(H)}\right] + 12 \qquad (1)$$

Where n = the number of atoms of that element. (Equations reproduced from Lodders 2003.) For example, to reproduce the published photospheric Si abundance value for the Sun of A(Si) = 7.54 we use:

$$A(Si) = \log\left[\frac{1x10^6}{2.884x10^{10}}\right] + 12 = 7.54 \qquad (2)$$

(n(Si)) and (n(H)) values from Lodders 2003. This value of 7.54 becomes the exponent for calculating solar [Si/H], such that $10^{7.54}$ = 3.5x10^7 Si atoms per mole.

The next step is to convert the element/H ratio for each star in our study to a decimal value relative to the solar value of 1. For example, the average of the reported [Si/H] for HIP 84720 b, is -0.225 (Gilli et al. 2006). Therefore, $10^{-0.225}$ = 0.596. Thus, this star contains roughly 60% the amount of Si in its photosphere per unit volume as the Sun. Next is to calculate the number of Si atoms per mole of the star's photosphere by multiplying the decimal value of the El/H ratio calculated in the previous step by the A(El)^{10} value calculated from the Lodders

(2003) data. To continue with our example; $0.596*(3.5*10^7) = 2.07*10^7$ Si atoms per mole in the photosphere of HIP 84720 b. Now we multiply by the atomic weight of Si: $Aw(Si) = (2.07*10^7)*28.0855 = 5.801*10^8$, which is the total weight of all Si atoms per mole in the photosphere of HIP 84720 b.

To arrive at the value of the bulk weight percent of elements that compose a rocky terrestrial planet orbiting any single HC star, the total weight of atoms for any single element as calculated above for Si is then divided by the sum of the values for all other atoms of interest, whose weights are determined in the same way, with the total normalized to 100:

$$E_w = \frac{A_w(El)}{[\sum_{i=\infty}^{i} A_w(El)]_t} * 100 \qquad (3)$$

where: $A_w(El)$ = the total weight of atoms of a single element per mole and $\Sigma A_w(El)_t$ = the total (t) sum of the weights of all atoms per mole. For HIP 84720 b the sum of the atomic weights for each of the nine pertinent elements = $2.1215*10^9$. So for HIP 84720 b, $[(5.801*10^8)/(2.1215*10^9)]*100 = 27.3427$. So for a terrestrial planet orbiting HIP 84720 b, it will be composed of around 27% Si by weight. Oxide weight percent values are then obtained with the equation:

$$O_{bw} = \left[\frac{E_w * O_w}{C_a * C_n}\right] \qquad (4)$$

Where E_w = weight % of elements, O_w = oxide molecular weight, C_a= cation atomic weight, and C_n = number of cations present in the oxide formula. For the above equation to be applicable, O must be available in sufficient abundance. The HC notes [H/O] between stars is rarely more than +/- 25%, and this difference does not prevent oxide formation per analysis.

So, for our Si example, we have our planetary Si weight percent of 27.3427, a Si oxide molecular weight of 60.0835, the Si (cation) atomic weight of

28.0855, and the number of cations present in the oxide formula, a value of 1 for SiO_2. Therefore; (27.3427*60.0835)/(28.0855*1) = 58.494. This value, 58.494, and the values for the other oxides, are then normalized to sum to 100. In this case, a terrestrial planet in orbit about HIP 84720b will have a bulk SiO_2 content of 35.6 wt. %.

The above procedures, performed for each oxide in our study, give an estimate of an exoplanet bulk composition. We next determine the size of the exoplanet core, using the partitioning of Fe between Earth's core and mantle, and from that, obtain a bulk composition for an exoplanet silicate mantle. The percent of Fe for the whole Earth is:

$$W_{Fe} = (C_{Fe} * C_x) + (M_{Fe} * M_x) \quad (5)$$

where W_{Fe}= the bulk concentration of Fe for the whole planet, C_{Fe} is the concentration of Fe in a planetary core, M_{Fe} = the concentration of Fe in an overlying silicate mantle, C_x= core mass fraction and M_x= the mantle mass fraction. C_x = 0.32.5 and M_x = 0.67.5, values rounded from those provided by Morgan & Anders (1980), and McDonough & Sun (1995). In this study all modeled planets retain this core/mantle mass fraction since both Earth and Venus possess this 1/3 to 2/3 division (Morgan & Anders 1980).

When more O is present in a planet, more FeO may be formed and retained in the mantle, which changes mantle chemistry. If the extent of the O availability seen between the terrestrial planets of the solar system, i.e. 18% for Mars and 3% for Mercury (Taylor 2013) are applied to the models in this study, some mineralogical change does occur, most notably in Ol, with differences up to 31%. However, as previously noted the variation in O abundance between stars rarely exceeds +/- 25% (Hinkle et al. 2014). This variation is only about 1/4 to 1/5 that seen in the O concentration gradient across the solar system. Thus, maximum

differences in minerology due to O abundance between stars should rarely exceed 8%, and most mineralogical variation will be on the order of 1-3%. The largest change expected amongst planets will therefore arise from concentration gradients, not stellar compositional variation. In future, eliminating this source of error will require applying each stellar [H/O] value to each mineral composition and core volume calculation.

These equations yield the size of a planet's core as a function of the relative abundance of Fe in the planet's bulk composition. Greater accuracy will be achieved by replacing all Fe fraction values with the estimated fraction of other elements thought to contribute to the core's composition. Therefore:

$$C_c = \sum_{i=1}^{x} = (C_{e1} + C_{e2} + \cdots) \quad (6)$$

Where C_c represents total estimated core composition as a sum of the mass fractions of Fe, Ni, Si, and so on.

For Earth, W_{Fe} = 33.26%, C_{Fe}= 88.0%, M_{Fe} = 6.3%, W_{Ni} = 1.83%, C_{Ni} = 5.15%, M_{Ni} = 0.196% (McDonough & Sun 1995; McDonough 2000). We assume that the physical processes of core and mantle differentiation, and thus the resultant difference in relative elemental abundances of the modeled planets operates in much the same way as it did during Earth's formation. The determining factor behind variations in elemental concentrations across the terrestrial planets in our own solar system are perhaps due to compositional gradients across the original protoplanetary disk (Moriarty et al. 2014). This means that our estimates of planet core sizes would more reflect those exoplanets that are a similar fractional distance from the star they orbit as the Earth, i.e. the predictability of this study may decrease for rocky planets which may have formed unusually close to or far from their host stars. Therefore, for this study such an equivalent orbital distance is assumed. Once properties of this study are applied to

known system architectures, specific analysis of those planetary orbits will be required.

To set the constant core mass fraction for each model exoplanet we use the "goal seek" function in Microsoft Excel to force these core mass fraction values to conform with the calculated iron concentration ratio between the planet's mantle and core. For example, by assuming that, like Earth, 89% of the Fe of a planet will be concentrated in its core, and the mantle retains roughly a 5.5% Fe composition, we force the core mass fraction to change relative to Earth as each planet has a different total amount of Fe in its bulk composition.

From this estimate, we calculate:

$$\Delta C = \frac{(P_{cm} - E_{cm}) * 100}{E_{cm}} \quad (7)$$

Where ΔC = percent change in mass of modeled planetary core relative to Earth's core, P_{cm} = modeled planet core mass fraction, and E_{cm} = Earth core mass fraction. We assume that the relative proportions of Fe and Ni between the core and depleted mantle will remain constant across all planetary models, such that 14 of 15 parts Fe accumulate in the Earth's core as this is the estimate for both Earth and Venus (Watt & Ahrens 1982) The above assumption can be removed by applying star-specific [O/H] values to each model. All remaining Fe is left to form FeO in the mantle and then combined with the remaining oxides forms the Bulk Silicate Mantle, or BSM for each model exoplanet (Table 1).

Similar to the situation with mantle minerology, O availability and thus rates of FeO production will affect final core size. As the largest variation in O abundance seen in our solar system results in a core twice the volume percent as Earth's core relative to the mantle, and this is about 5 times the average change in available O we see between other stars and the Sun, O abundance may have the ability to vary core size by up to 20%.

Table 1. A comparison of the oxide weight percent for the Sun derived from (Hinkle et al. 2014), and various other factors which both provide additional data and a check upon our own model output.

Planetary Mantle Oxide Wt % Estimate Comparison											
Oxide	SiO2	TiO2	Cr2O3	Al2O3	FeO	MgO	NiO	CaO	Na2O	SUM	
Sol Photosphere	46.48	0.15	0.757	3.28	10.6	31.9	2.77	2.74	1.38	100	Calculated
Carbonaceous Chondrite #1	51.15	0.16	0.59	2.37	10.7	28.87	3	2.28	0.85	100	Ringwood (1966)
Carbonaceous Chondrite #2	48.05	0.19	0.68	2.51	10.4	30.82	3.13	3.16	1.02	100	Ringwood (1966)
Carbonaceous Chondrite #3	50.63	0.16	0.68	2.35	9.74	31.32	2.17	2.02	0.92	100	Ringwood (1966)
Carbonaceous Chondrite #4	47.3	0.27	0.78	2.96	10.3	31.98	2.48	2.95	0.93	100	Ringwood (1966)
Carbonaceous Chondrite #5	46.39	0.17	0.61	3.58	10.4	32.43	2.55	2.77	1.05	100	Ringwood (1966)
Carbonaceous Chondrite #6	46.18	0.18	0.75	3.37	10.6	32.33	2.53	2.51	1.51	100	Ringwood (1966)
MORB #1	50.47	1.68	0	14.7	10.4	7.58	0	11.4	2.97	99.22	(Gale et al. 2013)
MORB #2	50.41	1.54	0	14.95	10.7	7.68	0	11.4	2.76	99.39	(Gale et al. 2013)
Bulk Crust #1	55.99	1.18	0	14.9	8.36	5.64	0	8.45	3.09	97.59	Calculated
Bulk Crust #2	54.76	1.12	0	15.38	8.35	6.04	0	8.88	2.98	97.5	
Bulk Crust #3	54.79	1.19	0	15.25	8.22	5.99	0	8.9	3.09	97.41	
Bulk Crust #4	55.96	1.11	0	15.03	8.49	5.69	0	8.43	2.98	97.68	
Depleted Mantle #1	44.71	0.13	0.57	3.99	8.03	37.71	0.24	3.17	0.28	98.83	(Workman & Hart 2005)
Depleted Mantle #2	44.9	0.16	0.41	4.26	8.02	37.3	0.24	3.45	0.22	98.96	(Walter 1998)
Depleted Mantle #3	44.5	0.16	0.31	3.59	8.1	39.22	0.25	3.44	0.3	99.87	(Walter 1998)
Depleted Mantle #4	45	0.2	0.38	4.55	8.05	37.8	0.25	3.55	0.36	100.1	(Walter 1998)
Depleted Mantle #5	45.2	0.22	0.46	3.97	7.82	38.3	0.27	3.5	0.33	100.1	(Walter 1998)
Bulk Silicate Earth #1	45.1	0.17	0.55	4.362	8.04	36.59	0.23	3.35	0.38	98.78	Calculated
Bulk Silicate Earth #2	45.24	0.19	0.396	4.649	8.03	36.21	0.23	3.64	0.32	98.91	
Bulk Silicate Earth #3	44.86	0.2	0.299	3.998	8.1	38.06	0.24	3.63	0.4	99.78	
Bulk Silicate Earth #4	45.38	0.23	0.367	4.917	8.07	36.68	0.24	3.72	0.45	100.1	
Bulk Silicate Mars #1	42.1	0	0	6.5	16	30.2	0	5.3	0	100.1	(Morgan & Anders 1979)
Bulk Silicate Mars #2	44.4	0.14	0.76	3.02	17.9	30.2	0	2.45	0.3	99.17	(Dreibus & Wanke 1985)
Bulk Silicate Mars #3	43.68	0	0	3.13	18.7	31.5	0	2.49	0.5	100	(Burtka & Fei 1997)
Bulk Silicate Mars #4	44.4	0	0	2.5	17.2	29.7	0	2.4	0	96.2	(Lodders & Fegley 1997)
Bulk Silicate Mars #5	47.5	0	0	2.5	17.7	27.3	0	2	0	97	(Sanloup et al. 1999)
Bulk Silicate Mars #6	51	0	0	2.5	11.4	27.3	0	2	0	94.2	(Sanloup et al. 1999)
Bulk Silicate Mars #7	47.1	0	0	2.5	16.9	29.1	0	1.9	0	97.5	(Mohapatra & Murta 2003)
Bulk Silicate Moon #1	53	0	0	4	11	29	0	3	0	100	(Kushov 1996)
Bulk Silicate Moon #2	51	0	0	4	10	32	0	3	0	100	(Kushov 1996)
Bulk Silicate Moon #3	53.5	0	0	2.5	12	29.7	0	2.3	0	100	(Kushov 1996)
Bulk Silicate Moon #4	50	0	0	6.3	10.4	28.5	0	4.8	0	100	(Kushov & Kronrod) 1998)
Bulk Silicate Moon #5	48.5	0	0	5.9	11.7	29.6	0	4.3	0	100	(Kushov & Kronrod) 1998)
Bulk Silicate Moon #6	54.13	0	0	5.1	13.8	22.94	0	4.07	0	100	(Lognonne et al. 2003)
Bulk Silicate Moon #7	50.2	0	0	4	17.6	25.2	0	3	0	100	(Lognonne et al. 2003)
Bulk Silicate Mercury	47.1	0.33	3.3	6.4	3.7	33.7	0	5.2	0.08	99.81	(Morgan & Anders 1980)
Bulk Silicate Venus	49.8	0.21	0.87	4.1	5.4	35.5	0	3.3	0.28	99.46	(Morgan & Anders 1980)

We then transform oxides for the BSM into mineral assemblages for each of the five distinct layers of Earth's mantle. The characteristics of which are described (Table 2) For each depth interval of the mantle, the oxide weights of SiO_2, Al_2O_3, FeOt, MgO, and CaO will be calculated from molecular fractions derived from numerical data provided by Hinkle et al. (2014).

Table 2 List of major mantle mineral components, their formulae, the elements comprising those minerals, and their common charges. In addition, a sequenced list of major mantle seismic discontinuities, and the theorized changes in mineralogy which accompany them. Balanced reactions are provided in table 7.

Mineral	Formula	Source
Olivine	$(Mg,Fe)_2SiO_4$	Deer, Howie, Zussman (3rd Ed.)
Clinopyroxine	$Ca(Mg,Fe)Si_2O_6$	Deer, Howie, Zussman (3rd Ed.)
Orthopyroxine	$(Mg,Fe)_2Si_2O_6$	Deer, Howie, Zussman (3rd Ed.)
Garnet	$(Mg,Fe,Ca)_3Al_2Si_3O_{12}$	Frost, (2008)
Wadsleite	$(Mg,Fe)_2SiO_4$	Frost, (2008)
Pyrope	$Mg_3Al_2Si_3O_{12}$	Deer, Howie, Zussman (3rd Ed.)
Majoritic Garnet	$Mg_3(MgSi)Si_3O_{12}$	Yu et al. (2011)
Ringwoodite	$(Mg,Fe)_2SiO_4$	Frost, (2008)
Perovskite	$CaSiO_3$	Frost, (2008)
Magnesiowüstite	(Mg,Fe)O	Frost, (2008)
Bridgemanite	$(Mg,Fe)SiO_3$	Wolf et al. (2015)

Element	Charge
O	2-
Si	4+
Fe	2+
Mg	2+
Ca	2+
Al	3+

Between 220 and 410 km OPX converts to garnet so OPX reduces and Garnet increases

$(Mg,Fe)_2Si_2O_6 \Rightarrow (Mg,Fe,Ca)_3Al_2Si_3O_{12}$

From 410 to 550 km CPX converts to garnet and dissapears. And Garnet begins to convert to majorite garnet

$Ca(Mg,Fe)Si_2O_6 \Rightarrow (Mg,Fe,Ca)_3Al_2Si_3O_{12}$

$(Mg,Fe,Ca)_3Al_2Si_3O_{12} \Rightarrow Mg_3(MgSi)Si_3O_{12}$

Starting at 550 km majorite garnet begins to produce CaSi Perovskite and is reduced.

$Mg_3(MgSi)Si_3O_{12} \Rightarrow CaSiO_3$

Beyond 660 km, majorite garnet dissapears entierly into bridgmanite + CaSi Perovskite. And Olivine (Ringwoodite) dissapears into magnesiowurstite and bridgmanite

$Mg_3(MgSi)Si_3O_{12} \Rightarrow (Mg,Fe)SiO_3 + CaSiO_3$

$(Mg,Fe)_2SiO_4 \Rightarrow (Mg,Fe)O + (Mg,Fe)SiO3$

To convert the calculated quantity of available oxides into mineral assemblages we follow the matrix transformation procedure of Thompson (1982) (Table 3).

Table 3. Our matrix transformation results for each of the five depth intervals of Earth's mantle. These same matrices are used to estimate the majority of both peridotite and pyroxenite planet models.

depth interval 0 - 220 km		Matrix Transform				
		SiO_2	$AlO_{1.5}$	FMO	CaO	Cation Sum
Olivine	$(Mg,Fe)_2SiO_4$	1	0	2	0	3
Clinopyroxine	$Ca(Mg,Fe)Si_2O_6$	2	0.1	1.2	0.7	4
Orthopyroxine	$(Mg,Fe)_2Si_2O_6$	1.9	0.1	1.9	0.1	4
Garnet	$(Mg)_3Al_2Si_3O_{12}$	3	2	2.7	0.3	8

	Olivine $(Mg,Fe)_2SiO_4$	Clinopyroxine $Ca(Mg,Fe)Si_2O_6$	Orthopyroxine $(Mg,Fe)_2Si_2O_6$	Garnet $(Mg)_3Al_2Si_3O_{12}$
SiO_2	-1.159668222	-0.176257128	1.420425091	-0.062208398
$AlO_{1.5}$	0.063763608	-0.124416796	-0.762052877	0.544323484
FMO	1.079834111	0.088128564	-0.710212545	0.031104199
CaO	1.4530845	1.798859513	-2.731985485	0.046656299

depth interval 220-410 km		Matrix Transform				
		SiO_2	$AlO_{1.5}$	FMO	CaO	Cation Sum
Olivine	$(Mg,Fe)_2SiO_4$	1	0	2	0	3
Clinopyroxine	$Ca(Mg,Fe)Si_2O_6$	1.9	0.05	1.45	0.6	4
Orthopyroxine	$(Mg,Fe)_2Si_2O_6$	2	0.1	1.8	0.1	4
Garnet	$(Mg)_3Al_2Si_3O_{12}$	3	2	2.5	0.5	8

	Olivine $(Mg,Fe)_2SiO_4$	Clinopyroxine $Ca(Mg,Fe)Si_2O_6$	Orthopyroxine $(Mg,Fe)_2Si_2O_6$	Garnet $(Mg)_3Al_2Si_3O_{12}$
SiO_2	-0.862745098	-0.147058824	1.151960784	-0.053921569
$AlO_{1.5}$	0.009803922	-0.367647059	-0.453431373	0.531862745
FMO	0.931372549	0.073529412	-0.575980392	0.026960784
CaO	0.480392157	1.985294118	-2.218137255	0.06127451

depth interval 410-520 km		Matrix Transform				
		SiO_2	$AlO_{1.5}$	FMO	CaO	Cation Sum
Wadsleite	$(Mg,Fe)_2SiO_4$	1	0	2	0	3
Clinopyroxene	$Ca(Mg,Fe)Si_2O_6$	2	0	1	1	4
Pyrope	$Mg_3Al_2Si_3O_{12}$	3	1	4	0	8
Majoritic Garnet	$Mg_3(MgSi)Si_3O_{12}$	4	0	4	0	8

	Wadsleite $(Mg,Fe)_2SiO_4$	Clinopyroxene $Ca(Mg,Fe)Si_2O_6$	Pyrope $Mg_3Al_2Si_3O_{12}$	Majoritic Garnet $Mg_3(MgSi)Si_3O_{12}$
SiO_2	-1	0	0	0.5
$AlO_{1.5}$	-1	0	1	-0.5
FMO	1	0	0	-0.25
CaO	1	1	0	-0.75

depth interval 520-660 km		Matrix Transform				
		SiO_2	$AlO_{1.5}$	FMO	CaO	Cation Sum
Ringwoodite	$(Mg,Fe)_2SiO_4$	1	0	2	0	3
Pyrope	$Mg_3Al_2Si_3O_{12}$	3	1	4	0	8
Majoritic Garnet	$Mg_3(MgSi)Si_3O_{12}$	4	0	4	0	8
Perovskite	$CaSiO_3$	1	0	0	1	2

	Ringwoodite $(Mg,Fe)_2SiO_4$	Pyrope $Mg_3Al_2Si_3O_{12}$	Majoritic Garnet $Mg_3(MgSi)Si_3O_{12}$	Perovskite $CaSiO_3$
SiO_2	-1	0	0.5	0
$AlO_{1.5}$	-1	1	-0.5	0
FMO	1	0	-0.25	0
CaO	1	0	-0.5	1

depth interval 660-2891 km		Matrix Transform			
		SiO_2	FMO	CaO	Cation Sum
Magnesiowüstite	(Mg,Fe)O	0	1	0	1
Bridgemanite	$(Mg,Fe)SiO_3$	1	1	0	2
Perovskite	$CaSiO_3$	1	0	1	2

	Magnesiowüstite (Mg,Fe)O	Bridgemanite $(Mg,Fe)SiO_3$	Perovskite $CaSiO_3$
SiO_2	-1	1	0
FMO	1	0	0
CaO	1	-1	1

Thompson's procedure for the algebraic transformation of mineral components is useful as a simple form of mass-balance where a single matrix transform may be applied to a wide range of starting compositions, eliminating the highly time-consuming process of determining a separate mass-balance equation for each stellar oxide composition and then attempting to estimate a best-fit mineral composition to solve that equation. In addition, for each depth in the mantle where increased pressures and temperatures force a change in minerology, a new matrix is created for that new set of minerals.

For this transformation, we determine the oxide components for each mineral in the uppermost depth layer of the mantle such that:

$(Mg,Fe)_2SiO_4^{Ol} = 1\ SiO_2 + 0\ AlO_{1.5} + 2\ FMO + 0\ CaO$

$Ca(Mg,Fe)Si_2O_6^{Cpx} = 2\ SiO_2 + 0.1\ AlO_{1.5} + 1.2\ FMO + 0.7\ CaO$

$(Mg,Fe)_2Si_2O_6^{Opx} = 1.9\ SiO_2 + 0.1\ AlO_{1.5} + 1.9\ FMO + 0.1\ CaO$

$(Mg)_3Al_2Si_3O_{12}^{Pyp} = 3\ SiO_2 + 2\ AlO_{1.5} + 2.7\ FMO + 0.3\ CaO$

In this model, we re-produce the transition demonstrated by Frost (2008) and Kaminsky (2012) where garnet gradually changes composition with pressure throughout the 220-410 and km depth interval and transition zone, as under greater pressure, garnet tends to become more Si rich. Garnet, being mostly pyrope ($Mg_3Al_2Si_3O_{12}$) mixed with 10% grossular ($Ca_3Al_2Si_3O_{12}$), and 15% almandine ($Fe^{2+}{}_3Al_2Si_3O_{12}$) near the top of the transition zone (Bernard et al. 2013), becomes fully majoritic ($Mg_4Si_4O_{12}$) at the base of the transition zone.

The oxide values may now be described in the 4x4 square array (Equation 8), and seen at the top of table 3:

$$\begin{bmatrix} 1 & 0 & 2 & 0 \\ 2 & 0.1 & 1.2 & 0.7 \\ 1.9 & 0.1 & 1.9 & 0.1 \\ 3 & 2 & 2.7 & 0.3 \end{bmatrix} \quad (8)$$

We then take the inverse of this matrix:

$$\begin{bmatrix} 1 & 0 & 2 & 0 \\ 2 & 0.1 & 1.2 & 0.7 \\ 1.9 & 0.1 & 1.9 & 0.1 \\ 3 & 2 & 2.7 & 0.3 \end{bmatrix}^{-1} = \begin{bmatrix} -1.16 & -0.18 & 1.42 & -0.06 \\ 0.06 & -0.12 & -0.76 & 0.54 \\ 1.08 & 0.09 & -0.71 & 0.03 \\ 1.45 & 1.80 & -2.73 & 0.05 \end{bmatrix} \quad (9)$$

Next, we use calculated mole fractions for each of the four oxides used in the matrix, which will be different for each modeled planet, but to continue with using HIP 84720 b, our calculated BSM mole fractions are: SiO_2 = 0.398, Al_2O_3 = 0.042, FMO = 0.529, CaO = 0.030. These form the row vector:

$$[\,0.398 \quad 0.042 \quad 0.529 \quad 0.030] \quad (10)$$

This row vector is then multiplied by the inverse matrix above, so:

$$[\,0.398 \quad 0.042 \quad 0.529 \quad 0.030\,] * \begin{bmatrix} -1.16 & -0.18 & 1.42 & -0.06 \\ 0.06 & -0.12 & -0.76 & 0.54 \\ 1.08 & 0.09 & -0.71 & 0.03 \\ 1.45 & 1.80 & -2.73 & 0.05 \end{bmatrix} \quad (11)$$

$$= [\,0.155 \quad 0.026 \quad 0.076 \quad 0.016\,] \quad (11\text{ b})$$

We then renormalize these values to sum to 100, obtaining:

$$56.9 + 9.4 + 27.8 + 5.9 = 100. \quad (12)$$

So, in this sample BSM, the average composition of the upper mantle is 56.9% Ol, 9.4% Cpx, 27.8% Opx, and 5.9% Gar.

This transformation procedure can produce nonsense results (e.g., negative values for a given mineral abundance) if the input BSM is not a positive sum of

the assumed minerals. For some exoplanet BSMs, such situations indeed arise, in which cases we determine the new mineral combination expected to form due to the oxide composition for that planet and that will yield a positive sum from the matrix transformation. For example, some high Si exoplanets are better described by a pyroxenite mantle, with or without a SiO_2 phase, and lacking Ol. If Ol is absent (or assumed so when its use leads to negative mineral abundances) we take advantage of a mathematical characteristic of matrices whereby setting the value of one entry to an arbitrarily large value will yield an inverse matrix with very small values, close to 0, as demonstrated in table 4.

Table 4. The matrix inverse process for the transformation of mineral components procedure by Thompson (1982) showing the initial matrix (top) and its inverse (bottom). By inserting a large value for SiO_2 in mineral "X", the values in the left column of its inverse are very small.

depth interval 0 - 410 km		Matrix Transform				
		SiO_2	$AlO_{1.5}$	FMO	CaO	Cation Sum
X	X	1000	0	0	0	1000
Clinopyroxine	$Ca(Mg,Fe)Si_2O_6$	2	0	1	1	4
Orthopyroxine	$(Mg,Fe)_2Si_2O_6$	2	0	2	0	4
Garnet	$(Mg)_3Al_2Si_3O_{12}$	3	2	3	0	8
		SiO_2	Clinopyroxine $Ca(Mg,Fe)Si_2O_6$	Orthopyroxine $(Mg,Fe)_2Si_2O_6$	Garnet $(Mg)_3Al_2Si_3O_{12}$	
	X	0.001	0	0	0	
	$AlO_{1.5}$	0	0	-0.75	0.5	
	FMO	-0.001	0	0.5	0	
	CaO	-0.001	1	-0.5	0	

This change effectively forces SiO_2, in our example (Table 4) to be partitioned among the remaining phases, and approximates the result obtained by a 4x4 initial matrix. The real-world meaning of this process is the creation of an unnaturally large molecule composed of a thousand SiO_2 units, i.e., $Si_{1000}O_{2000}$. Because such a molecule, if formed, would leave all other components (here, Mg+Fe, Ca and Al) bereft of Si, we effectively encourage SiO_2 to be partitioned

among Mg+Fe, Ca, and Al before making our hypothetical $Si_{1000}O_{2000}$ mineral. The end result is that we can generate a positive sum of three minerals with the 4th ($Si_{1000}O_{2000}$) calculated to be entirely negligible; the extra component is ignored until we have BSMs so SI-rich that our pyroxenite mineralogy yields negative values, in which case we allow SiO_2 to substitute for $Si_{1000}O_{2000}$ so yielding a quartz-saturated mantle. As the abundance of the minerals produced in this study can be compared to previous studies done on Earth-mantle compositions, it is simple to check relative accuracy (Table 5).

Table 5. The mathematical accuracy of our approach is tested by reproducing Earth's mineral compositions as estimated by earlier studies in the same way that we produce our exoplanet compositions.

Upper mantle (0-410 km)						
	Ol	Opx	Cpx	Garnet	sum	Source
wt. %	57	28	13		98	Workman & Heart 2005
wt. %	56	17	15	12	100	Frost 2008
wt. %	58	15	9	18	100	Kaminsky 2012
Average	57	20	12.3333333	15		
wt. %	56.90	27.84	9.40	5.86	100	Calculated
wt. %	56.02	26.72	10.82	6.44	100	Calculated
wt. %	63.91	19.45	11.53	5.12	100	Calculated
wt. %	58.26	23.34	11.35	7.05	100	Calculated
wt. %	58.41	24.62	11.21	5.76	100	Calculated
Average	58.70	24.40	10.86	6.05		
% error	2.89150607	18.0160971	13.5504404	148.090238		

Of course, the precise mineralogy varies with depth and to construct such a model, we must calculate the rate of increase of material density and gravitational acceleration as a function of depth. First, for ascertaining that this model can reproduce known characteristics of the Earth, values for the densities found at the top and bottom of Earth's inner core, outer core, lower mantle and upper mantle are acquired from Anderson (2007). To calculate bulk density of Earth, the equation

$$\rho_E = \sum_{i=1}^{4}\left(X_{Li} * \bar{\rho}_{Li}\right) \quad (13)$$

is used where $\bar{\rho}_{Li}$= average density of that layer, and X_{Li}= volume fraction of that layer out of Earth's total volume.

To calculate $\bar{\rho}_{Li}$ it is first necessary to determine the molar fraction of the end-members (E_{mx}), for each of the major mineral components hypothesized to compose that layer. The equation:

$$E_{mx} = \frac{Mi_x * A_{mx}}{A_{mx} + B_{mx}} \quad (14)$$

is used where Mi_x, = the mineral fraction in the mantle layer. A_{mx} = the mole fraction of the mineral endmember. B_{mx} = the mole fraction of the opposing endmember. This equation is used for determining the molecular fraction of each end member mineral in each mantle layer (Table 6).

Table 6. Mantle minerals, their end-members, and densities used in this study.

Depth Interval (km)	Mineral	End-Member	D (g/cm3)	Source
0-220 & 220-410	Olivine	Fo	3.222	Deer, Howie &
		Fa	4.392	Zussman (3rd ed.)
	Garnet	Prp	3.58	unless otherwise noted.
		Alm	4.32	
	Cpx	Di	3.22	
		Hd	3.56	
	Opx	En	3.21	
		Fs	3.96	
410-520	Wadsleite		3.84	Price et al. 1983
	Cpx	Di	3.22	
		Hd	3.56	
	Garnet	Ma	4.32	
		Prp	3.58	
520-660	Ringwoodite	Fo	3.691	Ahrens 1971
		Fa	4.845	Ahrens 1971
	Garnet	Ma	4.32	
	Perovskite		3.95	
660-2890	Magnesiowüstite		4.55	Speziale et al. 2007
	Bridgemanite		4.99	Wolf et al. 2015
	Perovskite		4.84	

For example, a planet orbiting HIP 84720 b will have an Ol fraction in its upper mantle of 0.452, a MgO mole fraction of 0.453, and a FeO mole fraction of 0.069. Therefore, (0.452*0.453)/(0.453+0.069) = 0.3917 for the fraction of Fo in Ol and Fa = (0.452*0.069)/(0.069+0.453)=0.0598. The sum of all mole fractions for the end-members of each mineral will = 1.

All exoplanets are set equal to one Earth volume, surface gravity is in direct proportion to planetary density, i.e. a density of 1.1 times the Earth's will result in a surface gravity of 1.1 g. Calculation of core radius is done with the equation:

$$C_r = \frac{3*C_v}{(4\pi)^{\frac{1}{3}}} \quad (15)$$

where C_v = core volume in km^3. Finally, pressures in Gpa for any depth in a planetary mantle may be calculated by

$$P = \frac{(\bar{P}*D*g_p)}{10^6} \quad (16)$$

where $\bar{P}$ = the Average pressure of each mantle layer and any shallower layers. D = depth in km, and g_p= planetary gravity calculated for that depth.

Convection of Earth's mantle is the primary driving force of plate tectonics (e.g. Morgan 1972; Parsons & McKenzie 1978; Gurnis 1988) and may be a requirement for long-term surface habitability (e.g. Gonzalez et al. 2001; Jackson et al. 2008). We attempted to gain a general understanding of mantle convection by calculating the Rayleigh number (Ra), as the Ra equation is commonly used in geophysics to determine the convective potential of a thermodynamic system. The Ra value is dimensionless and set such that if Ra > 10^3 a system will transfer heat via convection, and if Ra < 10^3, thermal conduction will prevail.

$$Ra = \frac{g\rho\alpha T D^3}{\kappa\mu} \quad (17)$$

where g = gravitational acceleration at the surface, ρ = density of the mantle in kg/M^3, and α = the coefficient of thermal expansion, where α range from 3x10^{-5} near Earth's surface down to 0.9x10^{-5} at the core mantle boundary (CMB) (Davies 2001); T = the average temperature of the mantle in K, a value that can only be calculated if the temperature at the CMB is known. The *T* at the CMB is calculated from Nomura et al. (2014):

$$T(K) = (-4439.749 + (1579.0383 * \ln(P))) + 273.15 \quad (18)$$

Where P = pressure in Gpa. D = the depth of the planetary mantle in meters; κ = the thermal diffusivity, and is taken as 10^{-6} near Earth's surface and at 1.5x10^{-6} at the CMB (Davies 1999).

κ is given in units of m^2/s. The average viscosity of the Earth's mantle (μ) is taken as 1x10^{22} Pascal seconds (Pas), with the upper mantle and transition zone being nearer 1x10^{21} Pas (Davies 2001, Burgmann & Dresen 2008). For reference, water at room temperature is generally set at 1 Pas where window glass at the same temperature is about 1x10^{27} Pas. Using Davies (2001), we calculate viscosity for our mantle models from:

$$\mu = \Delta\rho g R \tau \quad (19)$$

where $\Delta\rho$ = the difference between the mantle density and the density of any material above the surface of the planet, i.e. surface water, or atmospheric gasses should any exist. If not, then $\Delta\rho$ simply becomes ρ, which varies as a

function of depth. The g term = gravitational acceleration, and in this study R, viscous resistance, is set = to half the depth of the mantle in meters. The τ term is an empirical time function derived from observations of post-glacial crustal rebound rates (Mitrovica et al, 1994). This variable is the only one in this equation that is Earth-specific and likely to be the source of greatest error. For this study, τ is ≈ $1.5x10^{11}$ s (Davies 2001).

The presence or lack of water in the upper mantle can have a greater than two orders of magnitude effect on viscosity (Hirth & Kohlstedt 1996), likely having significant implications in regards to the ability for plate movement and subduction to occur, regardless of temperature and minerology. As this study does not account for various planetary surface conditions, such as the presence or lack of oceans, we assume a mantle water content of our planetary models equal to the Earth.

In addition to being a required component for calculating Ra, μ is also used when attempting to model rates of, and changes to, tectonic plate motion. The speed of plate motion is represented by the variable ν, which is calculated with the equation from Davies (2001):

$$\nu = D\left(\frac{g\rho\alpha T\sqrt{\kappa}}{4\mu}\right)^{2/3} \quad (20)$$

Where D = thickness of the mantle, g = the gravitational acceleration at the planet surface, ρ = density of the mantle in Kg/M^3, α = the coefficient of thermal expansion of the mantle material, T = the temperature of the mantle at the base of the lithosphere in °C, and κ = upper mantle thermal diffusivity.

In addition, other aspects of terrestrial planet thermodynamics are estimated. The depth of the 1300°C isotherm (base of the lithosphere) may be calculated from Davies (2001) by:

$$D = 2\sqrt{\kappa t} \quad (21)$$

where κ = thermal diffusivity of the upper mantle, and t = the age of the lithosphere in seconds. For this study the depth of Earth's isotherm is calculated as 112 km for oceanic crust with an age of 100Ma. With a lithosphere depth value, we estimate surface heat flux with the equation:

$$q = \frac{K\Delta T}{d} \quad (22)$$

Where *K* is the thermal conductivity of the lithosphere with a value of 3 W/m K, ΔT = a 1300°C temperature gradient through the boundary layer, and *d* is the value previously calculated isotherm depth.

All of the procedures and calculations described in this section are applied to re-create the Earth as best as we understand the planet's characteristics. Only once this form of ground-truthing has been successfully carried out, are any of these equations applied towards modeling characteristics of exoplanets. Here, model-specific calculated values for the constants described are used.

RESULTS

The metallicity of stars in the HC define the parameters of our calculated values. First is the size of the core for each modeled planet. The core does not simply increase or decrease relative to the overall size of a planet but is capable of varying from +17.2% to -51.2% by radius and from +5.5% to -21.3% by volume, relative to Earth, with no change in total planetary volume (figure 4).

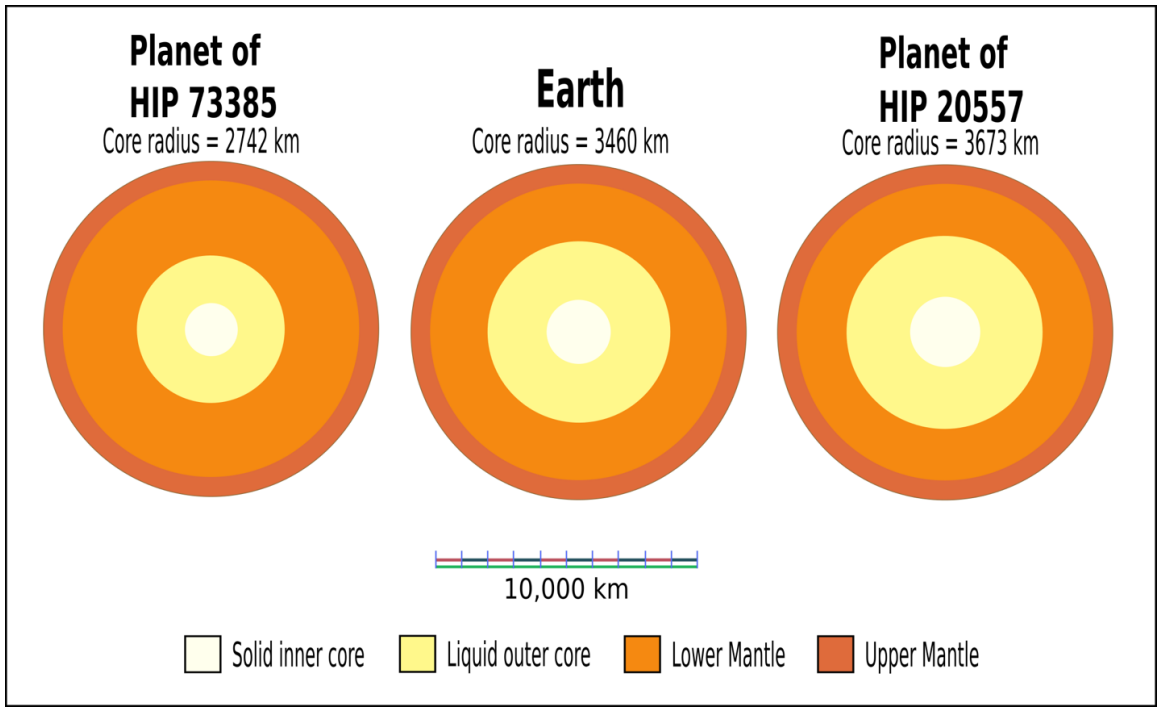

Figure 4. At center, a simplified cross section of the Earth to show relative thickness of major internal layers, compared to "end-member" states for earth-sized terrestrial planet interiors in terms of core volume.
Note: Among model runs, HIP 73385 produced the planet most depleted in heavy elements, generating a total core volume 21% less than Earth. HIP 20557 produced a planet with a total core volume of 5.5% greater than Earth.

The Earth is a somewhat heavy planet with a core that is larger than approximately 85% of all planets modeled. This result is in agreement with other studies (e.g. Unterborn et al. 2017). Because the size of a planet's core affects its ability to generate and retain heat, and the older a planet is, the cooler it becomes,

a planet with a larger core will be at a higher average temperature than a planet with a smaller core after the same amount of time. Therefore, the question arises if planets with core volumes significantly different from Earth's would behave similar to Earth in the geologic past or future in terms of planetary temperature. While this is the case, the relative temperature and representative planetary age difference is not a sufficiently significant factor on its own to extensively modify a planet's tectonic regime (figure 5).

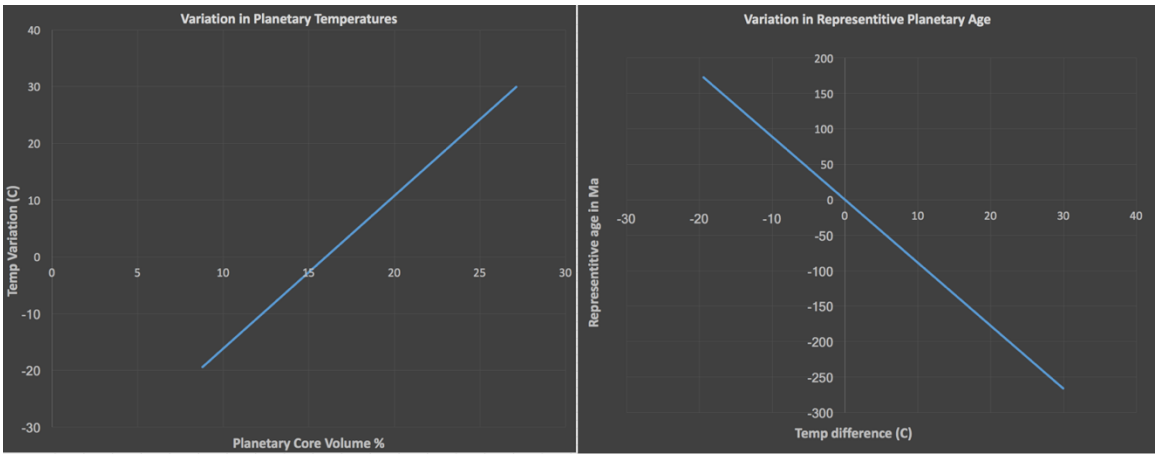

Figure 5. Comparisons of the related linear trends of predicted effects of core size on planetary temperature and the period of time of Earth's history to which that temperature corresponds.

Note: For example, a planet with a core volume of 20%, 4% greater than Earth's core, will have a temperature about 10 degrees centigrade higher than Earth, which is equivalent to Earth's average mantle temperature round 80 Ma ago. Planets with smaller cores than the Earth will have lower temperatures, equivalent to some point in our planet's future.

We also found that the volume of a planet's core positively correlates to mantle density, regardless of composition. This is because the core has a strong impact on planetary gravity and the increased g load compresses mantle material. Because a larger core results in a shallower mantle, such planets will never generate mantles with as high an absolute pressure and density. However, for any given depth as compared between two planet models, the planet with the larger core will have a higher density (figure 6).

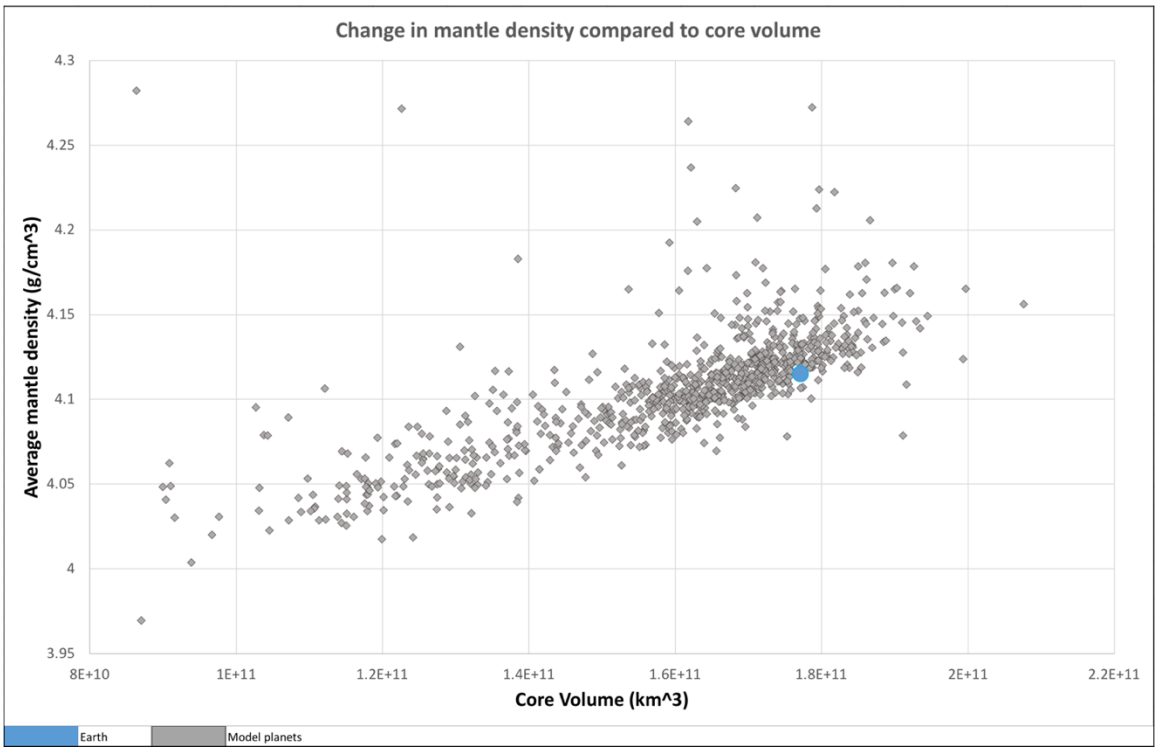

Figure 6. Correlation between core volume and mantle density as the latter increases due to higher pressures brought about by an increase in gravity as a result of a larger core.

Where Fe dominates planetary core properties, so too does Si in the mantle by acting as the limiting reagent in mantle chemistry. The presence and abundance of the defining mantle minerals Mws, Brg, Ol, and Opx, all primarily depend on the quantity of Si present.

Of the 893 models, 14% failed to be described by an Earth-like set of mineral proportions. As Ol does not play a major part in their compositions as it does in Earth. These fell into two distinct categories. The larger, representing 13% of the entire 893 total, are defined by very high Si concentrations; so high, that our model predicts that these will have pyroxene dominant mantle compositions, mostly Opx, (figure 7, upper right), or even quartz in extreme (0.2% of) cases. The rarer, second type of planet, represented by only 9 models, roughly 1% of the total, is characterized by exceptionally low levels of Si, meaning that these are incapable

of generating much if any of the Si rich pyroxenes. Their mantles become dominated by Ol, as it contains less Si when compared to the pyroxenes, and Mws, which contains no Si, with the pyroxenes nearly absent altogether (figure 7, bottom right). The rarity of such planets appears reasonable as only very metal poor stars will possess so little Si that their planets will not generate pyroxenes in their mantles (figure 7).

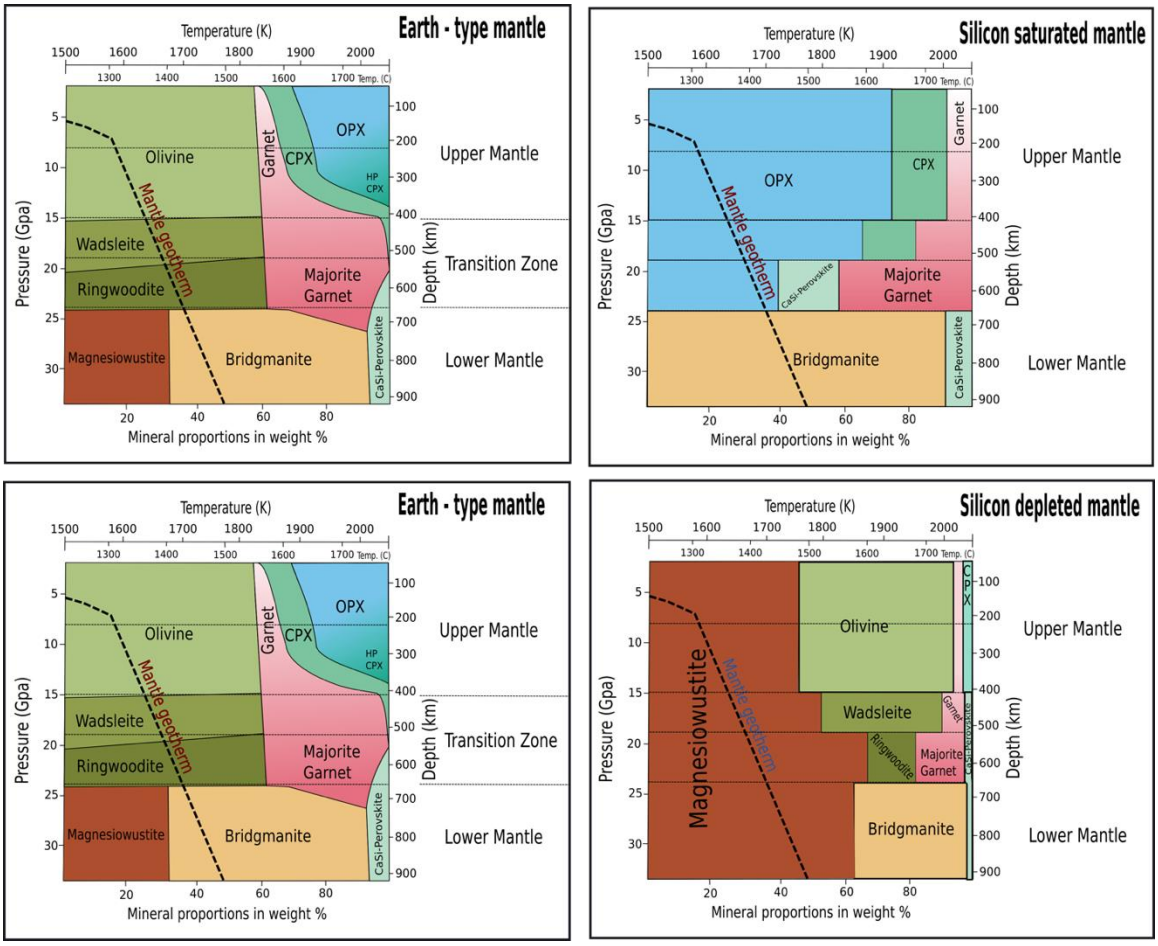

Figure 7. Representation of proportionality among mineral components of the Earth's mantle, compared to estimated mineral proportions in a Si saturated and Si depleted mantle as generated by our model.
Note: Earth-type mantle figure design modified from Kaminsky (2012).

For planets with mantle mineralogies like Earth, Brg, being the dominant phase in the lower mantle, will act as a control on the local rheological

environment. For Si poor planets, however, Mws could play an increased role in the lower mantle and, as our model indicates, could exist in quantity at depths equivalent to Earth's transition zone and upper mantle (figure 8).

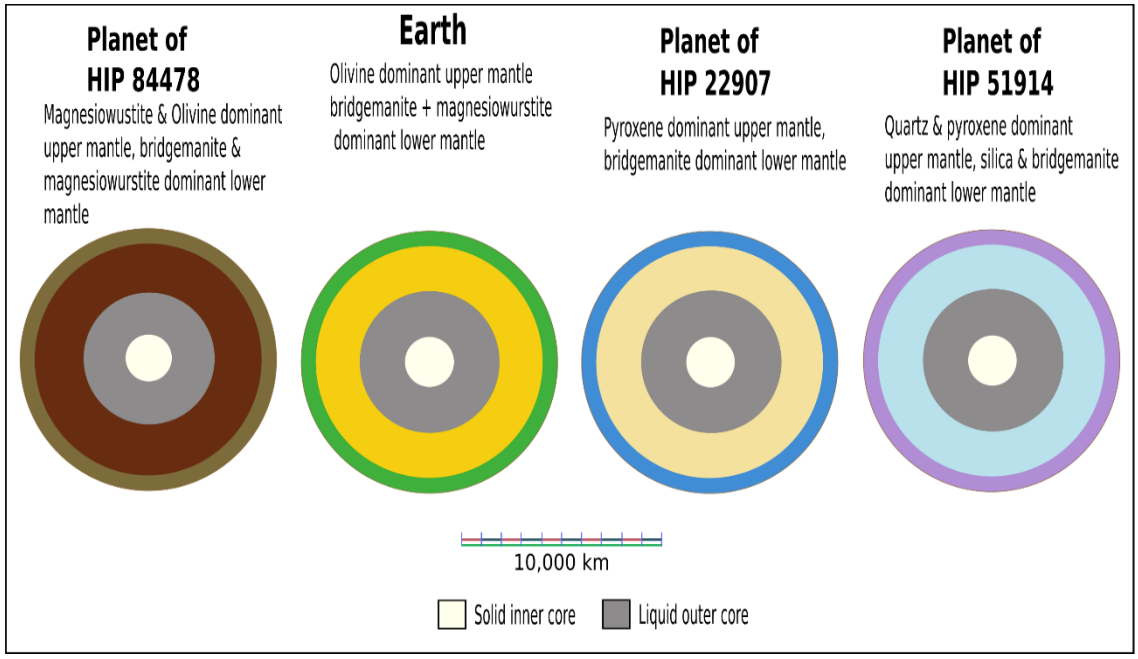

Figure 8. Cartoon similar to figure 4, a set of planetary "end-member" states as compared to Earth, but in this case showing maximum potential deviation in terms of Mws to Opx dominant mineral phases of the mantle across modeled planets. *Note*: Core size is nearly constant; we find little correlation between core parameters and mantle chemistry.

Also, mantle mineralogy and spectral class relationships show positive correlation between less luminous stars and mineralogical diversity. Nearly 23% of K class stars produced mantle models with < 0 or >1 mineral fraction values, while only 13% and 12% of G and F class stars respectively failed in the same way. This correlation is probably because less luminous stars represent larger proportions of the total galactic stellar population, and thus, are statistically more likely to cover a broader range of possible elemental compositions.

In addition, we attempted to determine if any noticeable correlations exist between any set of mantle minerals and stellar class. Most findings were

indeterminate. However, apparent weak correlations were found in some cases, such as demonstrated in figure 9. Cpx seems to increase slightly in abundance compared to wadsleyite for more luminous stellar classes, and the same may also be true for Cpx/Ol, Prv/Rwd, and Prv/Mws. However, these apparent correlations are small, and arguably within error.

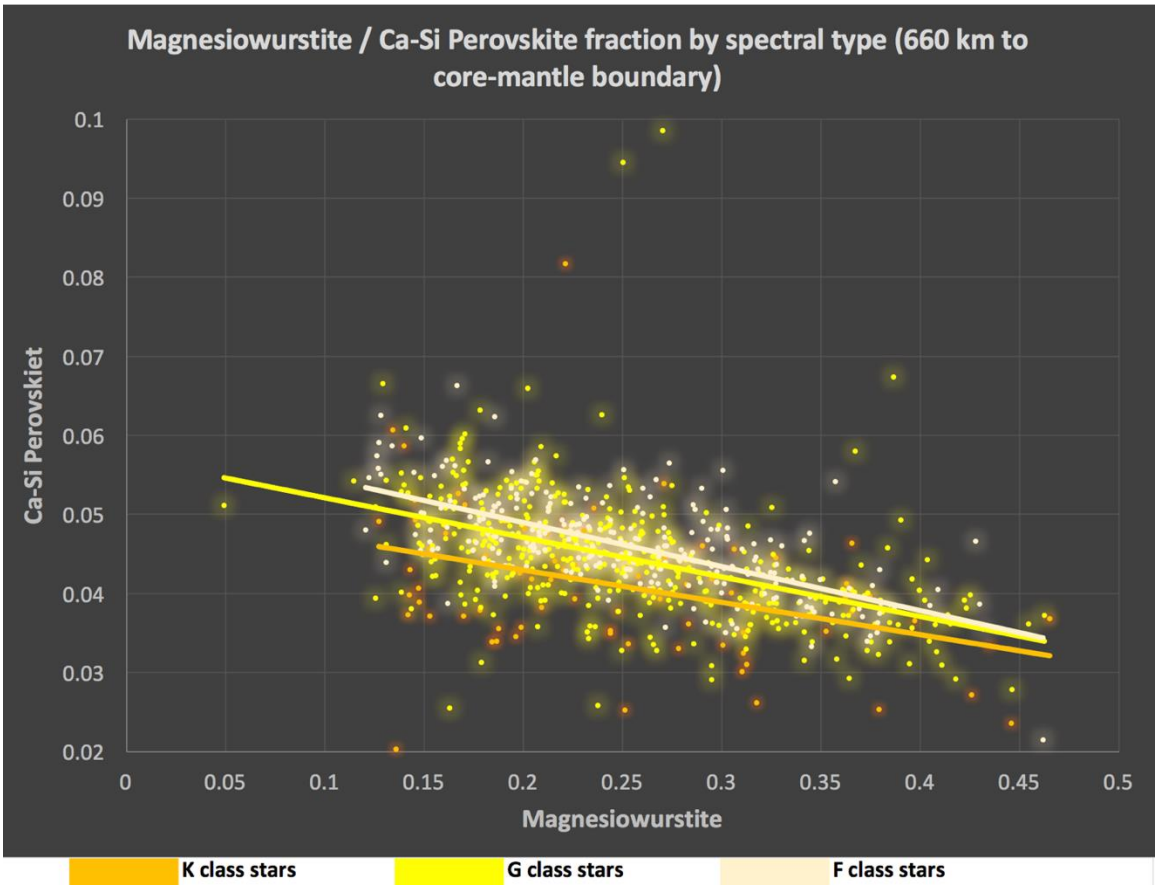

Figure 9. A sample chart demonstrating a case of potential weak correlation between increased Prv amounts relative to Mws formed in the mantles of planets of more massive stars.

The role of garnet among our models does not change as significantly as other mineral phases, because while its presence does depend on Si, it often incorporates many other less abundant elements such as Ti, Al, and Cr (Wood et al. 2013) and thus, as long as there is some Si present, Garnet-type structures will

form in the mantle. Garnet will also become more Si rich (Majoritic) in composition at increased depths (Wood et al. 2013), a process that we observe in our models regardless of Si abundance. The existence of garnet and its rate of increase in abundance do have an effect on mantle chemistry as noted in table 7.

Table 7. We provide estimates for the chemical reasoning behind the seismic discontinuities that define known transition zones of Earth's mantle using specific formulas we have derived for the garnets in our matrix calculations.

Depth (km)	Calculated mineral phase changes at mantle transition zones.
410	$Fm_2Si_2O_6^{Opx} + Ca_{1.5}Fm_{2.5}Al_2Si_3O_{12}^{Prp}$ Converts to: $Ca_{0.5}Fm_{3.5}Al_2Si_3O_{12}^{Maj} + CaFmSi_2O_6^{Cpx}$
	Note: The above process accounts for the decrease in abundance of Opx and increase of Garnet at this depth. The Ol to Wadslyite transition remains a constant in this equation.
550	$Ca_{1.5}Fm_{2.5}Al_2Si_3O_{12}^{Prp} + Ca_{0.5}Fm_{3.5}Al_2Si_3O_{12}^{Maj}$ Converts to: $Ca_{0.5}Fm_{3.5}Al_2Si_3O_{12}^{Maj} + CaSiO_3^{Prv}$
	Note: This accounts for the conversion of all previous garnet polymorphs to Majorite, and the creation of Ca-Si perovskite.
660	$Fm_2SiO_4^{Rwd} + Ca_{0.5}Fm_{3.5}Al_2Si_3O_{12}^{Maj}$ Converts to: $FmO^{Mws} + 5[MgSiO3]^{Brg}$
	Note: Ca-Si perovskite remains as a constant on both sides of the equation.

Note: The 220 km discontinuity is absent as it is not based on any change in mineral components.

Because planets with high Si do not form Ol in abundance, and are instead dominated by Opx, their mantle structure, in terms of the presence and depth of seismic discontinuities, will be distinct from the Earth. Similarly, changes to the atomic structure of Mws could also introduce discontinuities in the mantles of Si poor worlds distinct from Earth's. Because the depth at which a seismic discontinuity forms is dependent upon the pressure found at that depth, the changes in gravity due to the volume and mass of the core will cause any discontinuities present to appear at depths offset from where they would otherwise have formed had the planet possessed the same gravity as Earth (figure 10).

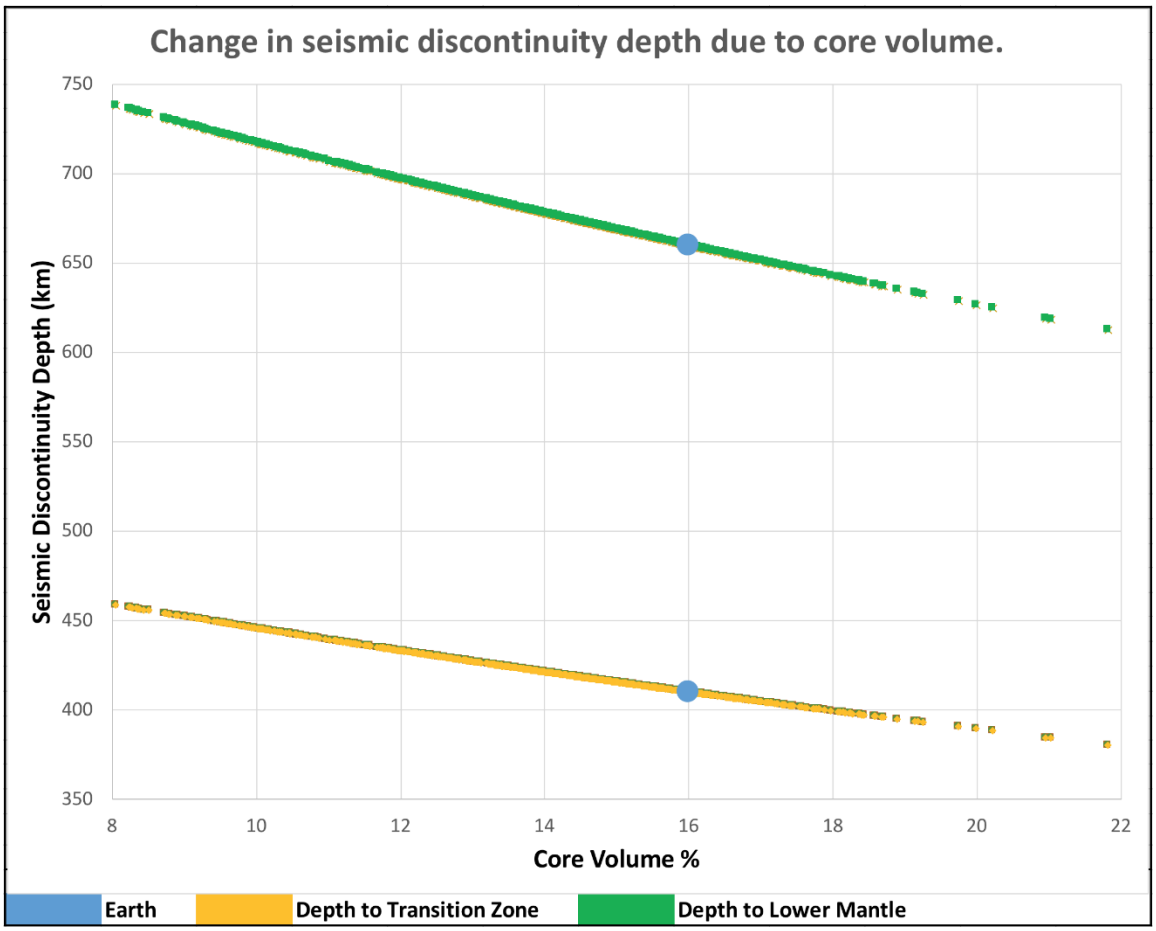

Figure 10. The seismic discontinuity which manifests in the Earth's mantle at a depth of 410 km may not appear until below 450 km in planets with small cores, and as shallow as around 350 km for the planets with the largest core volumes. *Note*: Likewise, the transition zone - lower mantle boundary will vary between 730 and 555 km in depth. Unlike the shallower, Ol-centric discontinuities, we expect the transition zone - lower mantle boundary to remain unaffected by increased pyroxene content.

This discontinuity comparison does not take into account mineralogical composition. Where planets have mineralogies that deviate from Earth's to a significant degree, a set of unique discontinuities will result. In the case of Si rich planets, the 220, 410, and 550 km discontinuities will become progressively weaker as Ol disappears at the expense of Opx. However, the 660 km discontinuity will remain strong (figure 11).

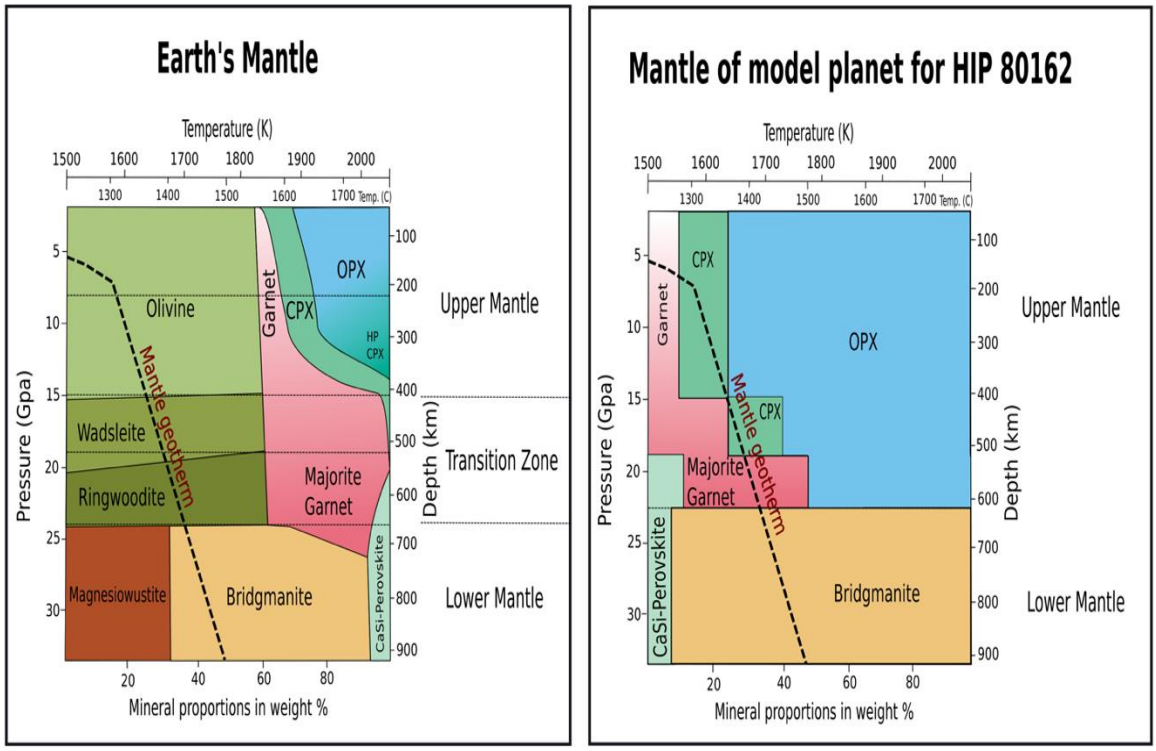

Figure 11. Here we compare Earth's mantle to our results for the characteristics of a mantle rich in Si, and a core comprising 20.25% of total planetary volume as compared to 16% for Earth's core.
Note: There is a lack of shallow discontinuities and decreased depth of the upper and lower mantle boundary. It is questionable whether a transition zone can be said to still exist for such a planet.

The behavior of mantle chemistry under the influence of high SiO_2 concentrations of >56 wt. % is unusual, and we suggest that under such conditions, Si becomes so overwhelming that pyroxene structures can no longer take up all available Si atoms. Opx is roughly limited to 55-56 wt.% SiO2, as is shown by ca. 700 Opx compositions (figure 12) This would imply that, given the pressures and temperatures involved, if a planet's mantle were to exceed this limit, the next more Si rich mineral structure that could form would be quartz. As quartz is structurally weak compared to the pyroxenes (Bürgmann & Dresen 2008), its presence would tend to reduce the rigidity of a mantle.

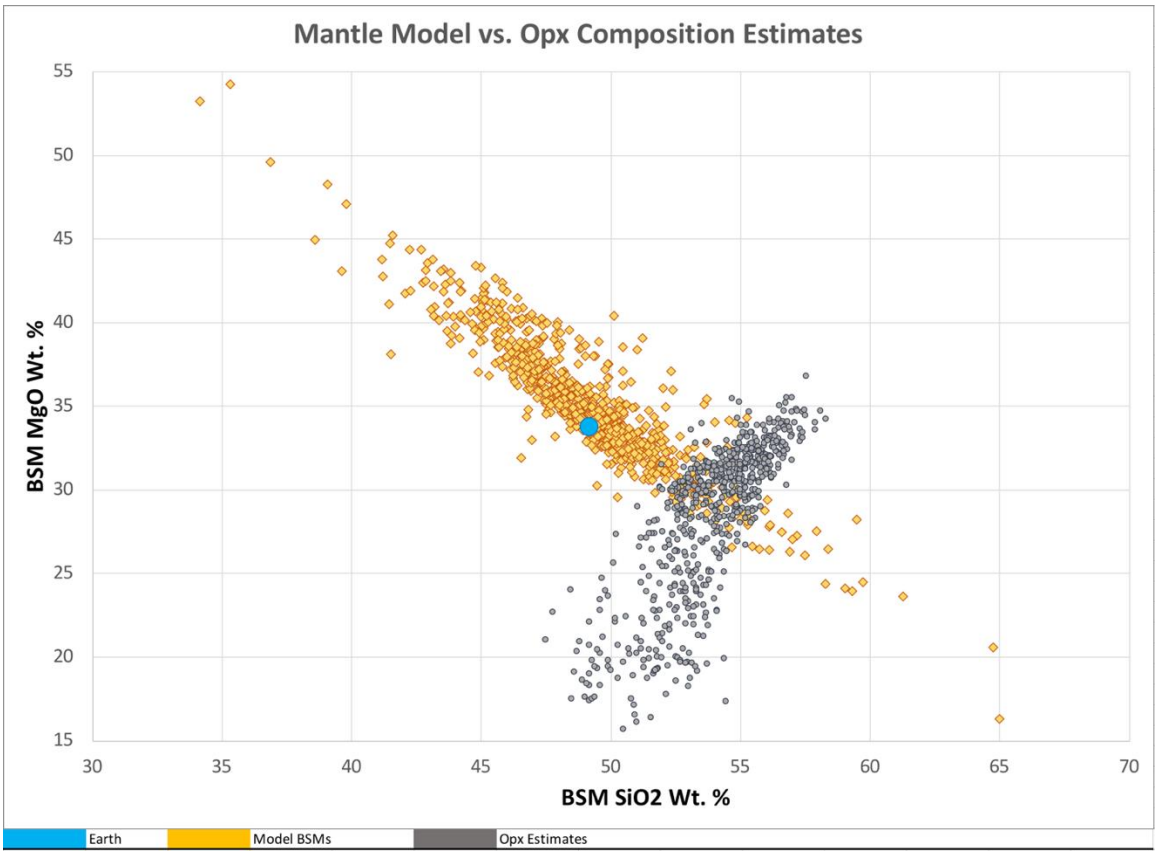

Figure 12. Overlaying Opx SiO_2 estimates atop our BSM models, clearly delineates which of our models possess sufficient Si to form quartz in the mantle. *Note*: Only the two right-most data points indicate planet mantles where quartz is the primary mantle mineral.

The structural rigidity, i.e. viscosity (μ) of planetary mantles is affected by mineral composition, primarily by Si content. The linked SiO_4 tetrahedral structures that form in greater abundances as the quantity of Si in the mantle increases, control the dominant mineral phase of the mantle (figure 13), (Unterborn et al. 2016, 2017). These provide a resistive force counter to the flow of mantle material due to the strong covalent bonds between the Si atoms, thus increasing viscosity and reducing mantle convection rates (Klein & Philpotts 2013).

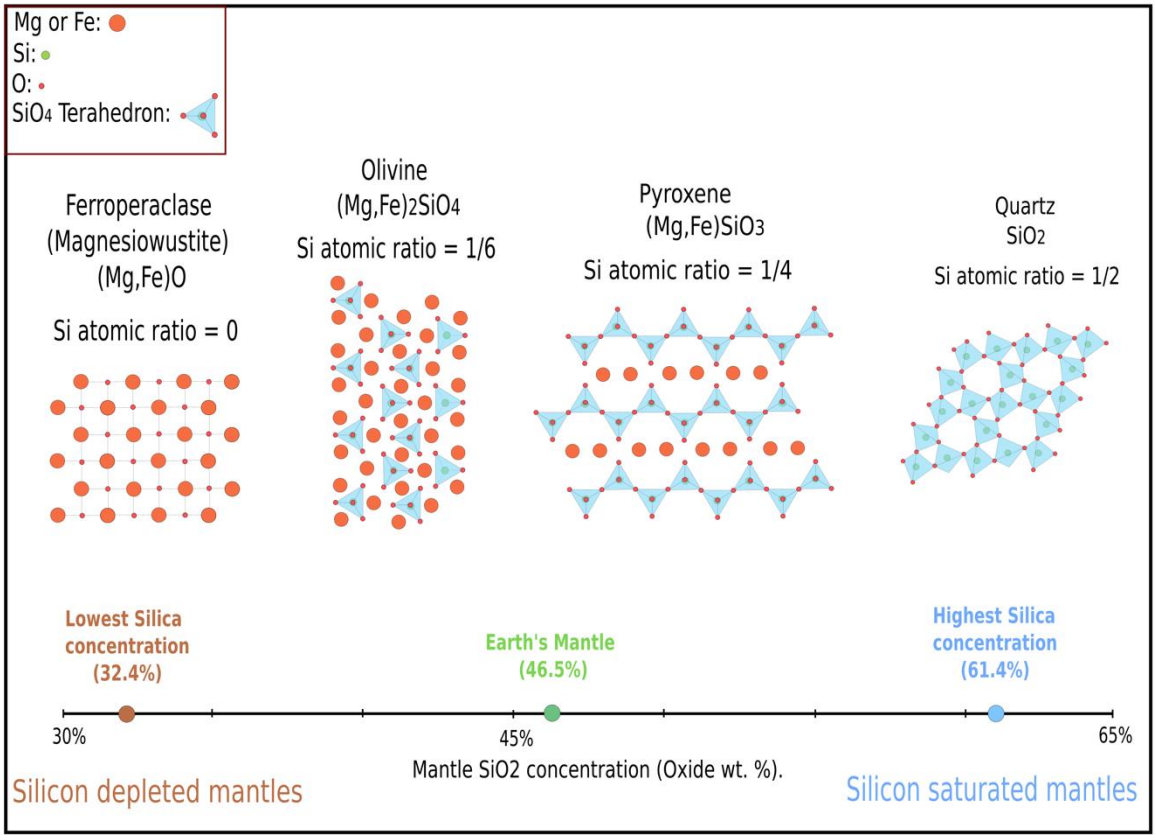

Figure 13. A 2-D representation of the atomic structures for the four major mineral components of planetary mantles, from Si depleted to Si saturated, showing the relative increase in the presence of SiO_4 tetrahedron.
Note: The mineral phases are shown relative to the type of mantle in which that phase is dominant. A Si depleted mantle is rich in Mws and Ol, Earth's mantle is dominated by Ol plus a pyroxene component, and a Si rich mantle is almost all pyroxene. Free quartz begins to appear in mantles with greater than 56% SiO_2 concentration.

The average mantle viscosity (μ) for the Earth is generally estimated to within an order of magnitude (Davies 2001), but it is even more difficult to constrain values of μ for other planets. We generally expect that as mantle compositions transition from mafic towards more felsic, i.e. moving from Mws, to Ol, to pyroxene dominant, μ will increase, and mantle convective potential will decrease. Mws is believed to be structurally much weaker than bridgmanite (Karato 1992), and would therefore act to reduce overall mantle viscosity for those planets lacking in Si (figures 14 & 15).

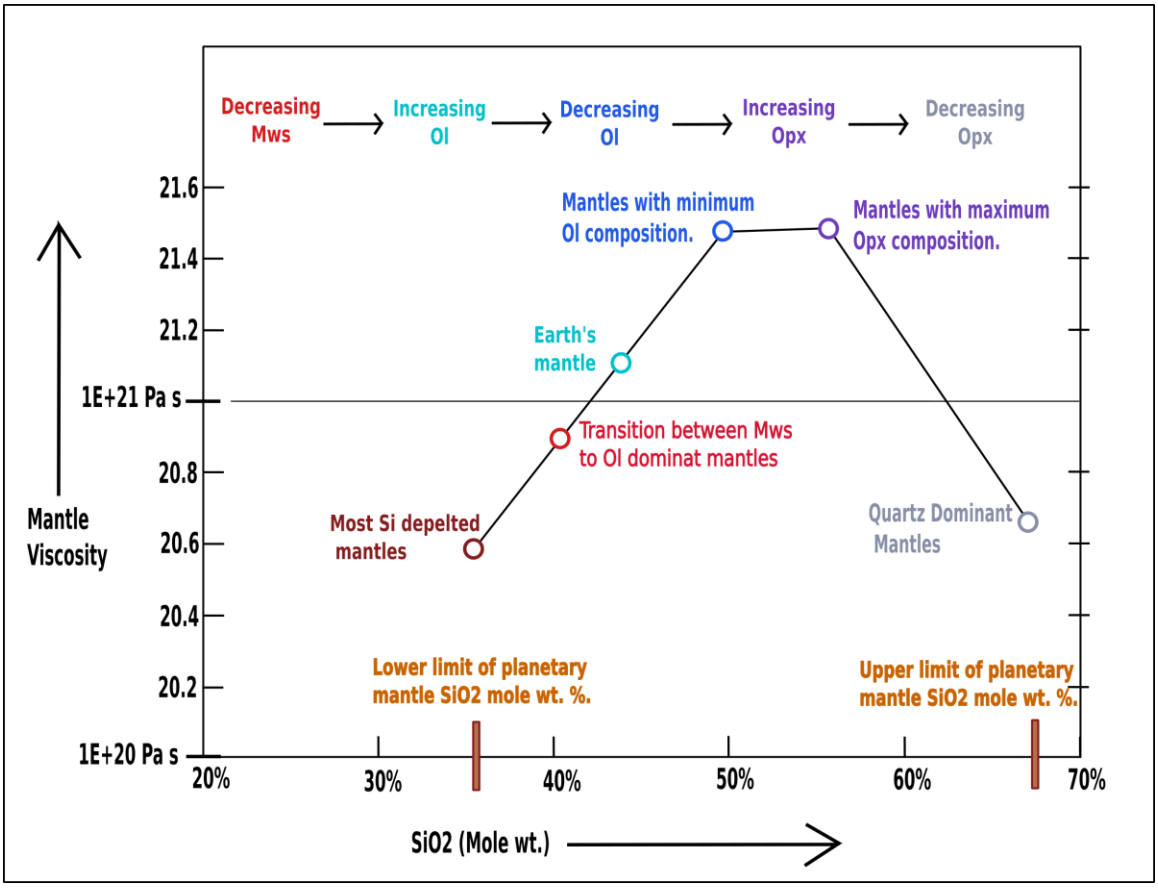

Figure 14. Cartoon diagram of predicted mantle viscosity trends.
Note: Earth's mantle, being Ol dominant but with significant pyroxene content, plots near a mid-way point for viscosity. The upper bound on mantle viscosity is determined by a composition of nearly 100% pyroxene. Error for mantle viscosity remains high, so this cartoon is more representative of predicted trends, not quantitative values.

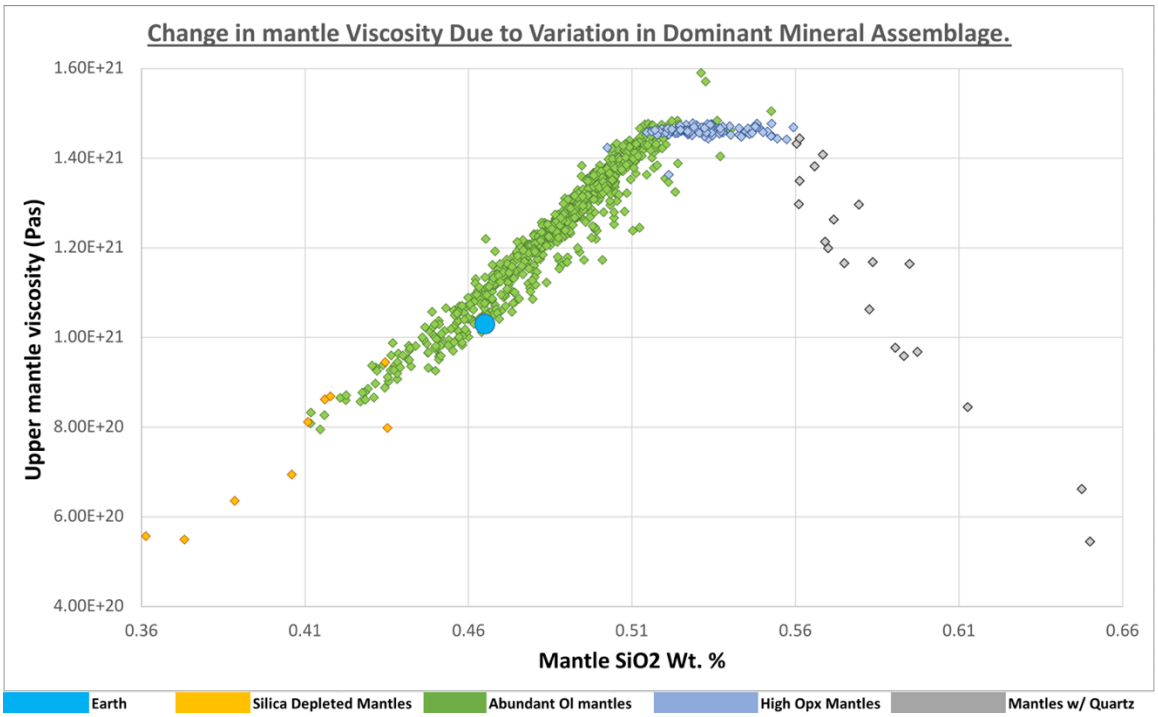

Figure 15. Plot of mantle viscosity for all 893 planetary mantle models using the same axes as figure 14.

Our modeling of relative concentrations of mineral species among mantle models shows that roughly 86% of these could be successfully modeled using the same 4x4 Ol-Cpx-Opx-Grt matrices first used to model Earth's mantle minerology. The remaining 14% of planetary mantles which were not successfully modeled by the first matrix transformation procedure, and which required the set of both low and high Si corrective matrices to be developed, were the ones for which a SiO_2 weight % of < 41% and > 52% was measured respectively. The upper division falls in line with the point of separation between peridotite and pyroxenite compositions. Therefore, we conclude that roughly 12% of planetary mantles will have an average pyroxenite composition due to high amounts of Si. Because these mantles no longer possess Ol in any relevant quantities, they show a distinct leveling-off trend at an average viscosity near to that of pure pyroxene.

As a way to define and investigate characteristics of our model mantles, we overlay their SiO_2 and MgO weight % values on a plot containing points representing the same oxide values for roughly 7,000 catalogued field samples. We divide the chart and its data points into separate bins, based on either axis (figure 16).

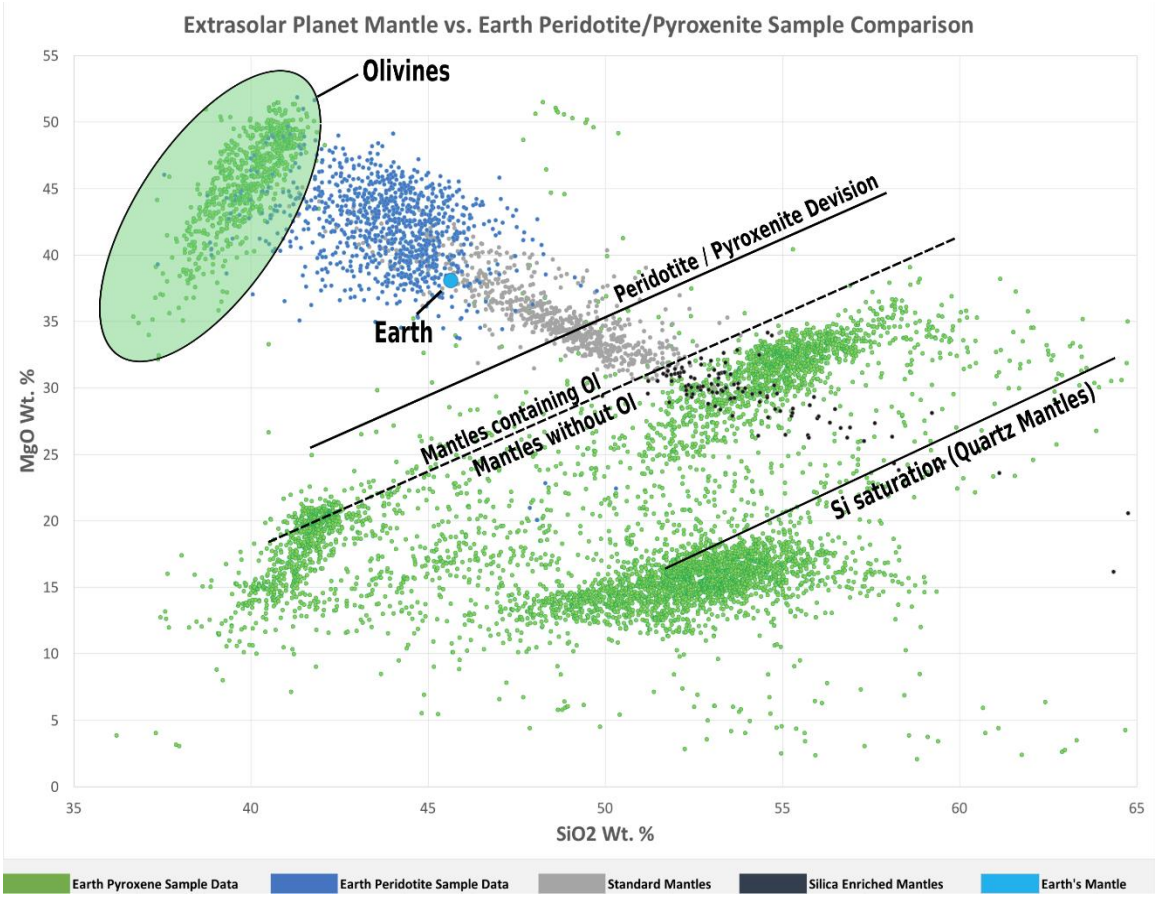

Figure 16. Comparison diagram of the average composition of all modeled exoplanet mantles with Earth-based pyroxenite and peridotite field sample composition data.

Note: Most modeled mantles fall into the pyroxenite category, with the majority of those being considered ultra-mafic, like the Earth, or mafic. Therefore, our planet compares to a peridotite in terms of BSM composition. A few mantles dominated by pyroxene fall into the intermediate classification, while none are intermediate-felsic.

A combination of both the X and Y axes allows for the diagonal separation between Peridotite and Pyroxenite categories. By overlaying our modeled planetary mantles on a plot that categorizes igneous rock samples based on SiO_2 content, we can make direct comparisons between mantle models and Earth based rock samples. For instance, we note that most of the model runs which worked with both the initial set of matrix transformation calculations and the matrices adjusted for high SiO_2 content fall into the mafic category. All the models which were produced using the matrices adjusted for low SiO_2 content plot in the same ultra-mafic region as the Earth based Ol samples. The few exceptions fall in a range that broadly covers the intermediate classification for igneous rocks. Therefore, we expect that these most extreme of Si enriched planets will possess bulk andesitic or dioritic compositions (figure 17).

Finally, our study allows us to shed some light on what types of planets will be better suited to a prolonged mobile-lid plate-tectonic regime, a geodynamical state considered most suitable for life. O'neill et al. 2016, make the case that planets are not bound to their initial tectonic state, and may transition from having a stagnant-lid to a mobile-lid and back again as the planet ages, providing a mobile-lid tectonic "window."

When and if this change in tectonic regime occurs in the planet's evolution depends on factors such as surface temperature (Weller & Lenardic 2018), Si, Na, and K content of the crust, (Unterborn et al. 2017), and mantle/lithosphere water content (e.g. Noack & Breuer 2014; O'neill et al. 2016). Also, of importance to a planet's tectonic state is the initial planet temperature, especially at the CMB and base of the lithosphere (O'neill et al. 2016).

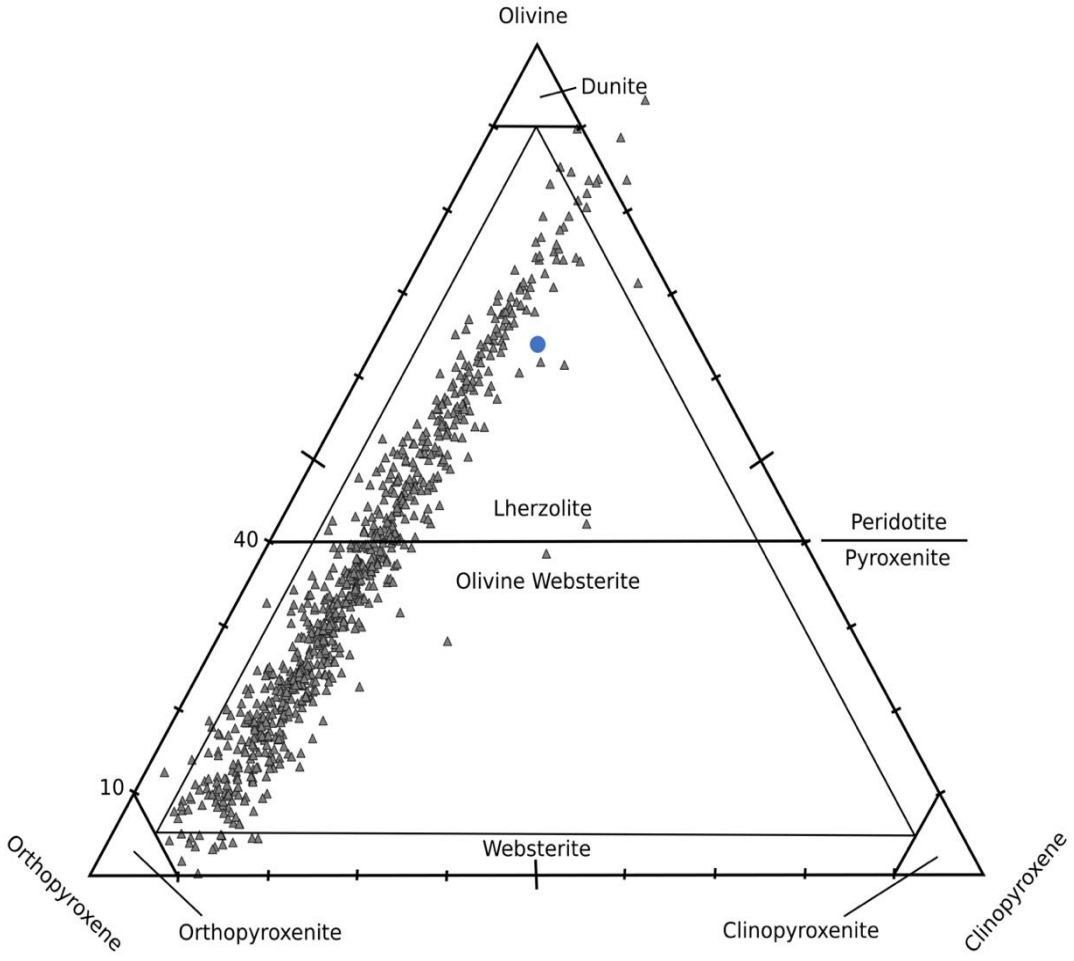

Figure 17. A companion diagram to figure 16 again showing that most planets are more pyroxenite dominant than Earth, but also that Earth may be slightly enriched in Cpx compared to most planets.

We find that there is a trend towards planets with larger cores and higher internal temperatures formed around more massive stars. It is precisely these worlds which are more vulnerable to experiencing a delayed onset of Earth-like mobile-lid conditions due to higher temperatures of formation, an issue when such massive stars may have main-sequence lifetimes of only half that of the sun or less (figure 18).

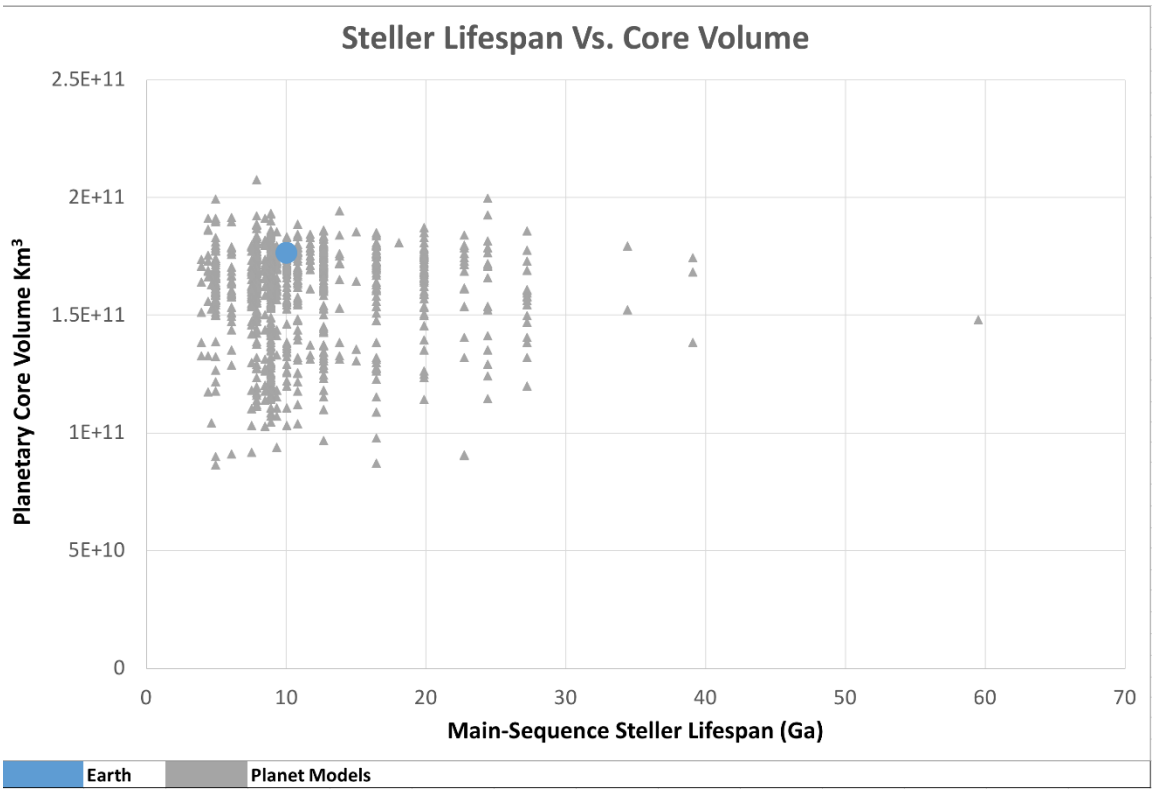

Figure 18. Graphical demonstration of more massive stars with shorter main-sequence lifetimes being more likely to host more massive planets with heavier cores.

In addition to previously mentioned properties, the planetary bulk temperature will play a role in viscosity, independent of mineral composition. As viscosity increases in inverse proportion to temperature, the ability for the mantle to convect will increase as temperature rises. As has been mentioned in regard to figure 5, the temperature changes we see will not alone be able to affect lithospheric subduction greatly since they are proportional to only about 100Ma of Earth's history, and as Earth's tectonic mode has not been observed to change within the past 100 Ma, we do not expect such small changes in temperature to have large tectonic effects. However, these changes in temperature, when coupled with a different minerology, may be capable of either exacerbating or subduing the mineralogical effect on lid type. An example is an apparent increase in the strength

of Opx also at temperatures <700ºC, indicating a stronger lithosphere, that is less able to deform (Yamamoto et al. 2008).

Though there is considerable uncertainty in regard to determining how much of a change in mantle characteristics relative to Earth would be required to terminate lithospheric subduction for any particular planet, certain specific trends may be anticipated (figure 19).

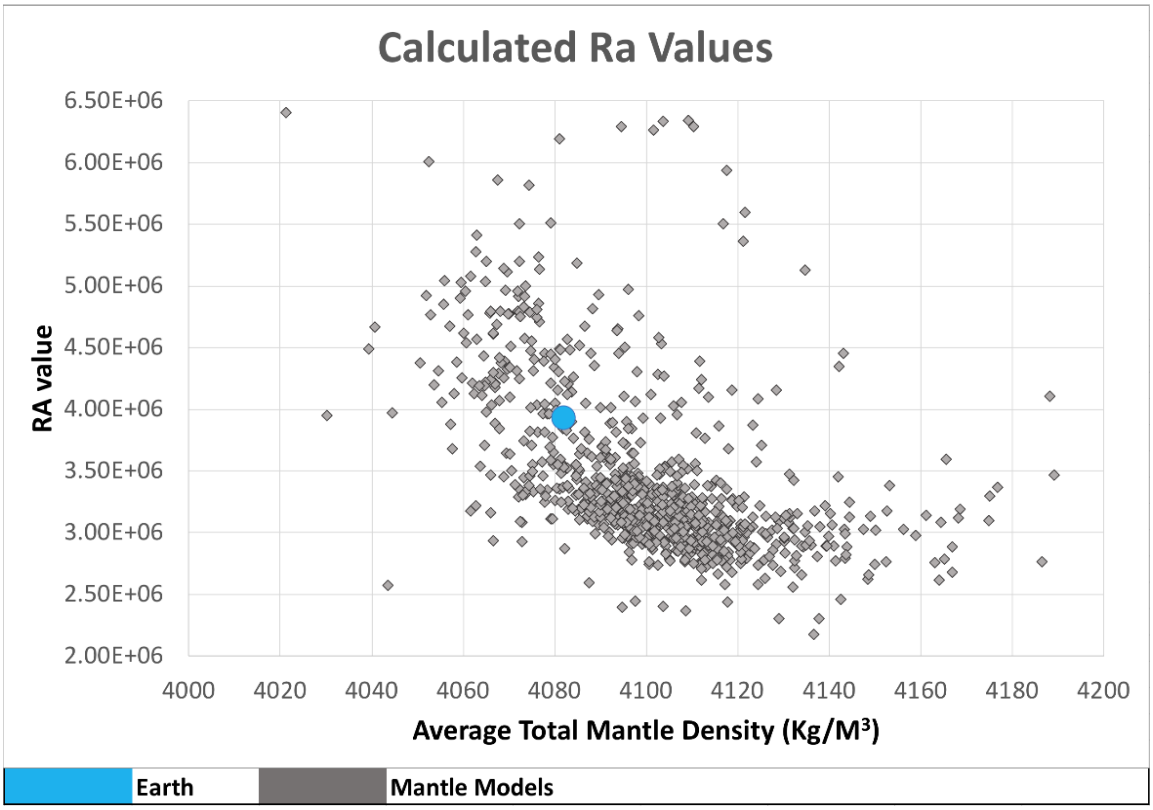

Figure 19. Rayleigh (RA) number values calculated for all exoplanet models using Davies (2001).
Note: No mineral composition is capable of forcing any planetary mantle into a state where convection might be hindered. A decrease in convective potential of three orders of magnitude would be required to do so.

As described in figures 13, 14, and 15, the proportion of SiO_2 to the total composition of a mantle may have effects on mantle rigidity (figure 20). SiO_2 composition should therefore be able to act as a proxy for viscosity, and when compared with mantle temperature, should produce a graph wherein a mobile-lid

regime will exist towards the upper left due to low SiO_2 and high temperature, and a stagnant lid regime will be located in the lower right due to high SiO_2 and low temp. Enhancing this trend is the possibility of higher Si content producing a lithosphere not only stronger, but lighter, and less easily subducted (Unterborn et al. 2017). A few mantle models hosting free quartz may plot in the upper right region, having very high SiO_2 but a mobile lid, although this is uncertain (figure 21). What remains to be determined is precisely what SiO_2 and temperature values correspond with which lid-type. This will be a component of future work.

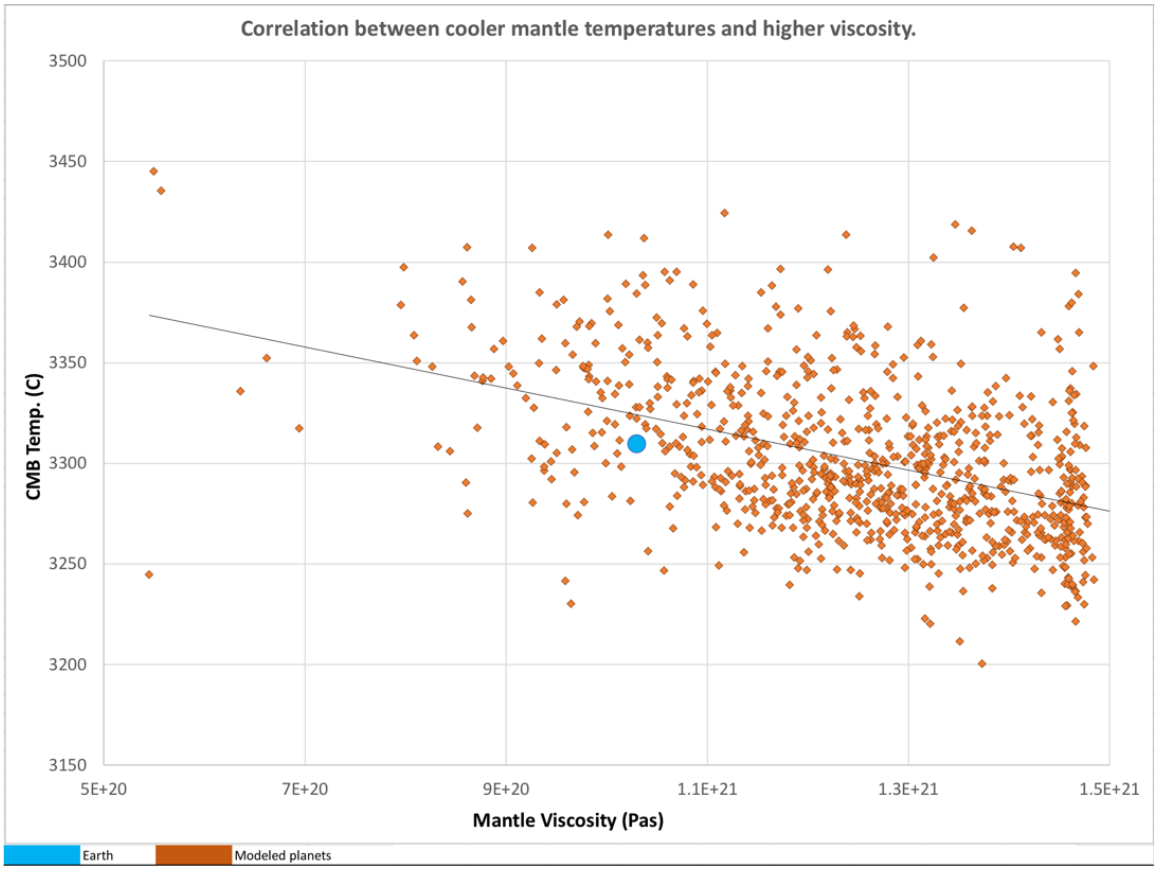

Figure 20. Inverse correlation between mantle viscosity and core-mantle boundary temperature.
Note: Here we use CMB temp as a general proxy for total planetary temperatures.

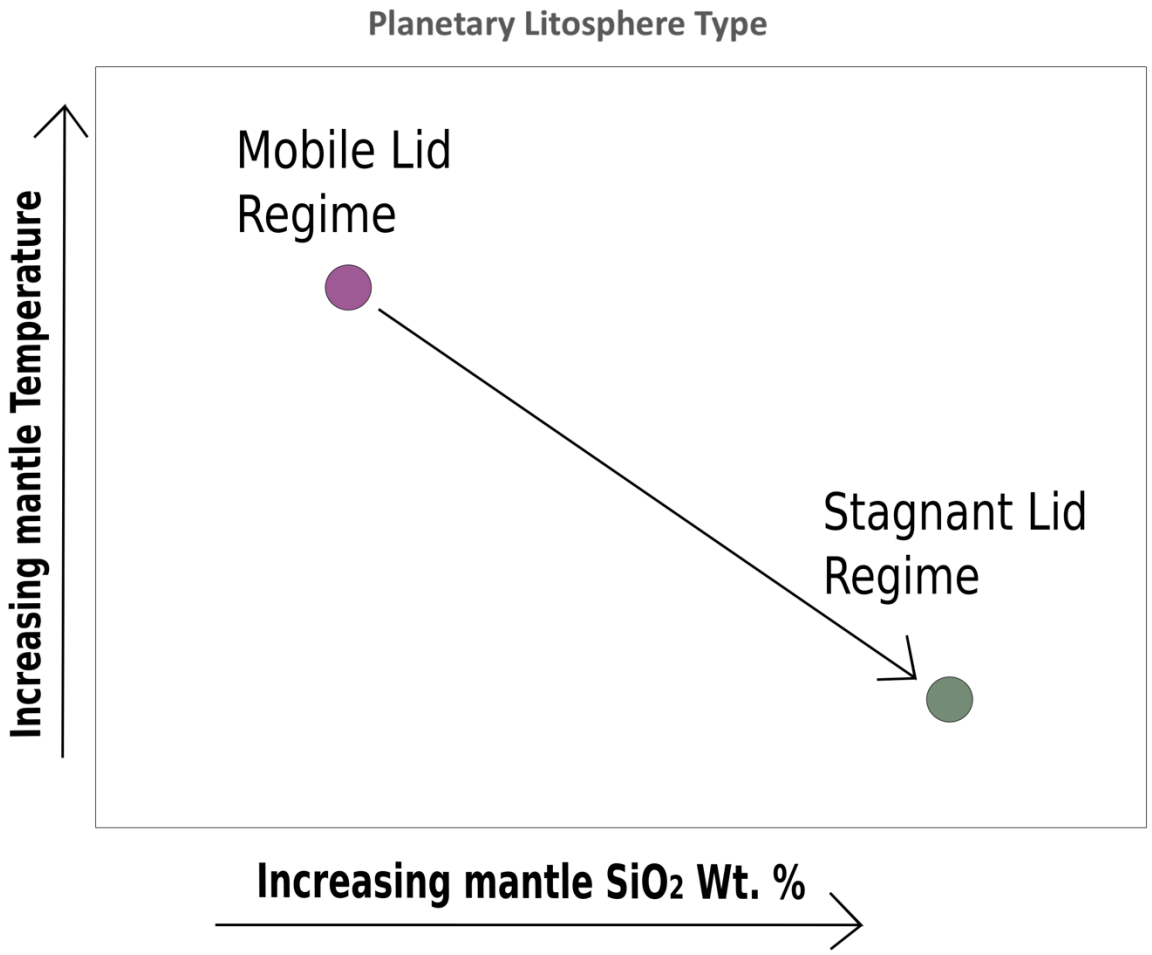

Figure 21. Expected format of a graph designed to represent which planets are more likely to experience either a mobile or stagnant lid based on the isolated parameter of SiO_2 wt. %.

Note: Though this parameter is not the most powerful determining factor governing tectonics, it should correspond in a predictable way. While a CMB temperature may be determined by the equation provided by Nomura et al. 2014 (equation 18). Changes to CMB temperature may be used as a proxy for equivalent differences in temperature at the top of the upper mantle since all models for this study possess mantle Ra values similar enough to the Earth, that strong mantle convection is not in doubt.

IMPLICATIONS

Improvements in the detection rate of extrasolar planets within the last two decades have resulted in sufficient discoveries via astronomical observation to begin the development of a galactic census in terms of the range of most common planetary properties, and overall system architectures to be found in the Milky Way. This however, is not all that can be achieved. By increasing our understanding of the ways different elemental compositions effect the geologic properties of planets, such as with this study and others, the galactic occurrence rate of more detailed planetary properties may be understood and used to strengthen the ability of scientists to classify planetary bodies of other stars in terms of minerology and rheology.

However, it is apparent that despite much progress towards these goals in recent years, current limited understanding of the rheological properties of minerals in the Earth's interior, especially Opx (Hansen & Warren 2015) remains a significant deficiency to overcome if real confidence in understanding extrasolar mantle and lithosphere behavior is to be developed.

Despite this lack of quantitative analyses, the common occurrence of planets more Si rich than the Earth would indicate that Earth is, on average, slightly Si poor, and thus may be, not uniquely, but more suited to stable plate tectonic crustal recycling than the average Earth-sized exoplanet. It is also seen that in cases of extreme Si under or over saturation that a very structurally weak mantle may result producing a tectonic regime very different that the one we are familiar with. Overall, then, the natural range in diversity among planetary characteristics remains quite high even if a large number of potential variables are held constant such as volume, surface temperature, relative orbital distance, and

presence of surface H_2O in quantity. In brief, Planetary lithophile elemental composition alone, irrespective of any other variable, can have a significant effect on planetary properties.

REFERENCES

REFERENCES

Anders, Edward, and Nicolas Grevesse. "Abundances of the elements: Meteoritic and solar." *Geochimica et osmochimica acta* 53.1 (1989): 197-214.

Anderson, Don L. *New theory of the Earth*. Cambridge University Press, 2007.

Anderson, Don L., and Robert L. Kovach. "The composition of the terrestrial planets." *Earth and Planetary Science Letters* 3 (1967): 19-24.

Asplund, Martin, Nicolas Grevesse, and A. Jacques Sauval. "The solar chemical composition." *Nuclear Physics A* 777 (2006): 1-4.

Asplund, Martin, et al. "The chemical composition of the Sun." *Annual Review of Astronomy and Astrophysics* 47 (2009): 481-522.

Batalha, Natalie M., et al. "Planetary candidates observed by Kepler. III. Analysis of the first 16 months of data." *The Astrophysical Journal Supplement Series* 204.2 (2013): 24.

Bethe, Hans Albrecht. "Energy production in stars." *Physical Review* 55.5 (1939): 434.

Bonanno, A., H. Schlattl, and L. Paternò. "The age of the Sun and the relativistic corrections in the EOS." *Astronomy & Astrophysics* 390.3 (2002): 1115-1118.

Borucki, William J., et al. "Characteristics of planetary candidates observed by Kepler. II. Analysis of the first four months of data." *The Astrophysical Journal* 736.1 (2011): 19.

Bradford A, Smith, and Terrile, Richard J. "A circumstellar disk around β Pictoris." *Science* 226.4681 (1984): 1421-1424.

Burbidge, E. Margaret, et al. "Synthesis of the elements in stars." *Reviews of modern physics* 29.4 (1957): 547.

Bürgmann, Roland, and Georg Dresen. "Rheology of the lower crust and upper mantle: Evidence from rock mechanics, geodesy, and field observations." *Annual Review of Earth and Planetary Sciences* 36 (2008).

Canup, Robin M., and Erik Asphaug. "Origin of the Moon in a giant impact near the end of the Earth's formation." *Nature* 412.6848 (2001): 708-712.

Chambers, John E. "Planetary accretion in the inner Solar System." *Earth and Planetary Science Letters* 223.3 (2004): 241-252.

Clark, Sydney P., and A. E. Ringwood. "Density distribution and constitution of the mantle." *Reviews of Geophysics* 2.1 (1964): 35-88.

Clayton, R. N. "Genetic relations among meteorites and planets." *IAU Colloq. 39: Comets, Asteroids, Meteorites: Interrelations, Evolution and Origins*. 1977.

Condie, Kent C., and Victoria Pease, eds. *"When did plate tectonics begin on planet Earth?"*. Vol. 440. Geological Society of America, 2008.

Connelly, James N., et al. "The absolute chronology and thermal processing of solids in the solar protoplanetary disk." Science 338.6107 (2012): 651-655.

Coradini, A., G. Magni, and C. Federico. "Formation of planetesimals in an evolving protoplanetary disk." *Astronomy and Astrophysics* 98 (1981): 173-185.

Davies, Geoffrey F. "Dynamic Earth: plates, plumes and mantle convection." (2001): 620-621.

Davies, Geoffrey F. "Gravitational depletion of the early Earth's upper mantle and the viability of early plate tectonics." *Earth and Planetary Science Letters*243.3 (2006): 376-382.

Drake, Michael J., and Kevin Righter. "Determining the composition of the Earth." *Nature* 416.6876 (2002): 39-44.

Dressing, Courtney D., et al. "The mass of Kepler-93b and the composition of terrestrial planets." *The Astrophysical Journal* 800.2 (2015): 135.

Dziewonski, Adam M., and Don L. Anderson. "Preliminary reference Earth model." *Physics of the earth and planetary interiors* 25.4 (1981): 297-356.

Ehrenfreund, Pascale, et al. "Extraterrestrial amino acids in Orgueil and Ivuna: Tracing the parent body of CI type carbonaceous chondrites." *Proceedings of the National Academy of Sciences* 98.5 (2001): 2138-2141.

Elser, Sebastian, Michael R. Meyer, and Ben Moore. "On the origin of elemental abundances in the terrestrial planets." *Icarus* 221.2 (2012): 859-874.

Engle, Scott G., and Edward F. Guinan. "Red dwarf stars: ages, rotation, magnetic dynamo activity and the habitability of hosted planets." *arXiv preprint arXiv:1111.2872* (2011).

Fischer-Gödde, Mario, and Thorsten Kleine. "Ruthenium isotopic evidence for an inner Solar System origin of the late veneer." *Nature* 541.7638 (2017): 525-527.

Fitoussi, Caroline, and Bernard Bourdon. "Silicon isotope evidence against an enstatite chondrite Earth." *Science* 335.6075 (2012): 1477-1480.

Frost, Daniel J., et al. "Experimental evidence for the existence of iron-rich metal in the Earth's lower mantle." *Nature* 428.6981 (2004): 409.

Frost, Daniel J. "The upper mantle and transition zone." *Elements* 4.3 (2008): 171-176.

Gaetani, Glenn A., and Timothy L. Grove. "Partitioning of moderately siderophile elements among olivine, silicate melt, and sulfide melt: constraints on core formation in the Earth and Mars." *Geochimica et Cosmochimica Acta* 61.9 (1997): 1829-1846.

Gilli, G., et al. "Abundances of refractory elements in the atmospheres of stars with extrasolar planets." *Astronomy & Astrophysics* 449.2 (2006): 723-736.

Goldstein, J. "The fate of the Earth in the red giant envelope of the Sun." *Astronomy and Astrophysics* 178 (1987): 283-285.

Gonzalez, Guillermo, Donald Brownlee, and Peter Ward. "The galactic habitable zone: galactic chemical evolution." *Icarus* 152.1 (2001): 185-200.

Grevesse, N., and A. J. Sauval. "Standard solar composition." *Space Science Reviews* 85.1-2 (1998): 161-174.

Gurnis, Michael. "Large-scale mantle convection and the aggregation and dispersal of supercontinents." *Nature* 332.6166 (1988): 695-699.

Hales, A. L., K. J. Muirhead, and J. M. W. Rynn. "A compressional velocity distribution for the upper mantle." *Tectonophysics* 63.1-4 (1980): 309-348.

Halliday, Alex N. "Mixing, volatile loss and compositional change during impact-driven accretion of the Earth." *Nature* 427.6974 (2004): 505-509.

Hama, Juichiro, and Kaichi Suito. "Thermoelastic models of minerals and the composition of the Earth's lower mantle." *Physics of the Earth and Planetary Interiors* 125.1 (2001): 147-166.

Hart, Stanley R., and Alan Zindler. "In search of a bulk-Earth composition." *Chemical Geology* 57.3-4 (1986): 247- 267.

Helffrich, George R., and Bernard J. Wood. "The Earth's mantle." *Nature*412.6846 (2001): 501-507.

Herschel, John Frederick William. "XXXI. On the Absorption of Light by Coloured Media, and on the Colours of the Prismatic Spectrum exhibited by certain Flames; with an Account of a ready Mode of determining the absolute dispersive Power of any Medium, by direct experiment." *Earth and Environmental Science Transactions of The Royal Society of Edinburgh* 9.2 (1823): 445-460.

Hansen, Lars N., and Jessica M. Warren. "Quantifying the effect of pyroxene on deformation of peridotite in a natural shear zone." *Journal of Geophysical Research: Solid Earth* 120.4 (2015): 2717-2738

Hinkel, Natalie R., et al. "Stellar abundances in the solar neighborhood: the hypatia catalog." *The Astronomical Journal* 148.3 (2014): 54.

Hirth, Greg, and David L. Kohlstedt. "Water in the oceanic upper mantle: implications for rheology, melt extraction and the evolution of the lithosphere." *Earth and Planetary Science Letters* 144.1-2 (1996): 93- 108.

Hofmann, Albrecht W. "Chemical differentiation of the Earth: the relationship between mantle, continental crust, and oceanic crust." *Earth and Planetary Science Letters* 90.3 (1988): 297-314

Howard, Andrew W., et al. "Planet occurrence within 0.25 AU of solar-type stars from Kepler." *The Astrophysical Journal Supplement Series* 201.2 (2012): 15.

Hull, S. D., et al. "The Potential for Plate Tectonics about Sun-like Stars in the Galaxy as Controlled by Composition." *AGU Fall Meeting Abstracts*. 2016.

Iben Jr, Icko. "Stellar Evolution. VI. Evolution from the Main Sequence to the Red-Giant Branch for Stars of Mass 1 M_ {sun}, 1.25 M_ {sun}, and 1.5 M_ {sun}." *The Astrophysical Journal* 147 (1967): 624.

Inoue, Toru, et al. "Elastic properties of hydrous ringwoodite (γ-phase) in Mg 2 SiO 4." *Earth and Planetary Science Letters* 160.1 (1998): 107-113.

Isacks, Bryan, Jack Oliver, and Lynn R. Sykes. "Seismology and the new global tectonics." *Journal of Geophysical Research* 73.18 (1968): 5855-5899.

Jackson, Brian, Rory Barnes, and Richard Greenberg. "Tidal heating of terrestrial extrasolar planets and implications for their habitability." *Monthly Notices of the Royal Astronomical Society*391.1 (2008): 237-245.

Jackson, Matthew G., and A. Mark Jellinek. "Major and trace element composition of the high 3He/4He mantle: Implications for the composition of a nonchonditic Earth." *Geochemistry, Geophysics, Geosystems* 14.8 (2013): 2954-2976.

Javoy, Marc, et al. "The chemical composition of the Earth: Enstatite chondrite models." *Earth and Planetary Science Letters* 293.3 (2010): 259-268.

Jones, John H., and Michael J. Drake. "Geochemical constraints on core formation in the Earth." (1986).

Jones, Rhian H., et al. "Formation of chondrules and CAIs: Theory vs. observation." *Protostars and planets IV* 1 (2000): 927.

Jura, M., et al. "A pilot search for evidence of extrasolar earth-analog plate tectonics." *The Astrophysical Journal Letters* 791.2 (2014): L29.

Kaminsky, Felix. "Mineralogy of the lower mantle: A review of 'super-deep'mineral inclusions in diamond." *Earth-Science Reviews* 110.1-4 (2012): 127-147.

Karato, Shun-ichiro. "On the Lehmann discontinuity." *Geophysical Research Letters* 19.22 (1992): 2255-2258.

Khodachenko, Maxim L., et al. "Coronal mass ejection (CME) activity of low mass M stars as an important factor for the habitability of terrestrial exoplanets. I. CME impact on expected magnetospheres of Earth-like exoplanets in close-in habitable zones." *Astrobiology* 7.1 (2007): 167-184.

Kirchhoff, Gustav, and Robert Bunsen. "Chemische analyse durch spectralbeobachtungen." *Annalen der Physik* 186.6 (1860): 161-189.

Klein, Cornelis, and Anthony R. Philpotts. *Earth materials: introduction to mineralogy and petrology*. Cambridge University Press, 2013.

Korenaga, Jun. "On the likelihood of plate tectonics on super-Earths: does size matter?." *The Astrophysical Journal Letters* 725.1 (2010): L43.

Kruijer, Thomas S., et al. "Lunar tungsten isotopic evidence for the late veneer." *Nature* 520.7548 (2015): 534-537.

Kudoh, Y., T. Inoue, and H. Arashi. "Structure and crystal chemistry of hydrous wadsleyite, Mg 1.75 SiH 0.5 O 4: possible hydrous magnesium silicate in the mantle transition zone." *Physics and Chemistry of Minerals* 23.7 (1996): 461-469.

Lehmann, Inge. "Velocities of longitudinal waves in the upper part of the Earth's mantle." *Annales de géophysique*. Vol. 15. 1959.

Laplace, Pierre-Simon. Exposition du système du monde, (1796)

Lineweaver, Charles H., and José A. Robles. "Comparing the Chemical Compositions of the Sun and Earth." *Bioastronomy 2007: Molecules, Microbes and Extraterrestrial Life*. Vol. 420. 2009.

Lodders, Katharina. "Solar system abundances and condensation temperatures of the elements." *The Astrophysical Journal* 591.2 (2003): 1220.

Lodders, K., H. Palme, and H-P. Gail. "4.4 Abundances of the elements in the Solar System." *Solar system*. Springer Berlin Heidelberg, 2009. 712-770.

Lovell, Bernard. "Sporadic outbursts of red dwarf stars." *Quarterly Journal of the Royal Astronomical Society* 12 (1971): 98.

Marcy, Geoffrey W., et al. "Occurrence and core-envelope structure of 1–4× Earth-size planets around Sun-like stars." *Proceedings of the National Academy of Sciences* 111.35 (2014): 12655-12660.

Marshall, J., and J. Cuzzi. "Electrostatic enhancement of coagulation in protoplanetary nebulae." *Lunar and Planetary Science Conference*. Vol. 32. 2001.

McDonough, William F., and S-S. Sun. "The composition of the Earth." *Chemical geology* 120.3-4 (1995): 223-253.

McDonough, William F., Edited by Roman Teisseyre, and Eugeniusz Majewski. "in, Earthquake Thermodynamics and Phase Transformations in the Earth's Interior." (2000).

McKeegan, K. D., et al. "The oxygen isotopic composition of the Sun inferred from captured solar wind." *Science* 332.6037 (2011): 1528-1532.

McSween, Harry Y. "Are carbonaceous chondrites primitive or processed? A review." *Reviews of Geophysics* 17.5 (1979): 1059-1078.

Megessier, C. "Evolution of the silicon abundance distribution in the atmosphere of magnetic BP and AP stars." *Astronomy and Astrophysics* 138 (1984): 267-274.

Mena, E. Delgado, et al. "Chemical clues on the formation of planetary systems: C/O versus Mg/Si for HARPS GTO sample." *The Astrophysical Journal* 725.2 (2010): 2349.

Minnaert, M. "On the continuous spectrum of the corona and its polarisation. With 3 figures.(Received July 30, 1930)." *Zeitschrift fur Astrophysik* 1 (1930): 209.

Mitrovica, J. X., J. L. Davis, and I. I. Shapiro. "A spectral formalism for computing three-dimensional deformations due to surface loads: 2. Present-day glacial isostatic adjustment." *Journal of Geophysical Research: Solid Earth* 99.B4 (1994): 7075-7101.

Mohorovičić, Andrija. "Potresod 8." (1909): 1-56.

Moore, Kevin, and Pascale Garaud. "Main Sequence Evolution with Layered Semiconvection." *The Astrophysical Journal* 817.1 (2016): 54.

Morgan, William Wilson, Philip Childs Keenan, and Edith Kellman. "An atlas of stellar spectra, with an outline of spectral classification." *Chicago, Ill., The University of Chicago press [1943]* (1943).

Morgan, W. Jason. "Deep mantle convection plumes and plate motions." *AAPG bulletin* 56.2 (1972): 203-213.

Moriarty, John, Nikku Madhusudhan, and Debra Fischer. "Chemistry in an evolving protoplanetary disk: effects on terrestrial planet composition." *The Astrophysical Journal*787.1 (2014): 81.

Morton, Timothy D., and John Asher Johnson. "On the low false positive probabilities of Kepler planet candidates." *The Astrophysical Journal* 738.2 (2011): 170.

Noack, Lena, and Doris Breuer. "Plate tectonics on rocky exoplanets: Influence of initial conditions and mantle rheology." *Planetary and Space Science* 98 (2014): 41-49.

Nomura, Ryuichi, et al. "Low core-mantle boundary temperature inferred from the solidus of pyrolite." *Science* (2014): 1248186.

O'Neill, Craig, et al. "A window for plate tectonics in terrestrial planet evolution?". *Physics of the Earth and Planetary Interiors*255 (2016): 80-92.

O'neill, C., and A. Lenardic. "Geological consequences of super-sized Earths." *Geophysical Research Letters* 34.19 (2007).

O'Neill, C., A. M. Jellinek, and A. Lenardic. "Conditions for the onset of plate tectonics on terrestrial planets and moons." *Earth and Planetary Science Letters* 261.1 (2007): 20-32.

Opher C. M. Kay, and M. Kornbleuth. "Probability of CME Impact on Exoplanets Orbiting M Dwarfs and Solar-Like Stars." *The Astrophysical Journal* 826.2 (2016): 195.

O'Rourke, Joseph G., and Jun Korenaga. "Terrestrial planet evolution in the stagnant-lid regime: Size effects and the formation of self-destabilizing crust." *Icarus* 221.2 (2012): 1043-1060.

Parsons, Barry, and Dan McKenzie. "Mantle convection and the thermal structure of the plates." *Journal of Geophysical Research: Solid Earth* 83.B9 (1978): 4485-4496

Payne, Cecilia Helena. "Stellar Atmospheres; a Contribution to the Observational Study of High Temperature in the Reversing Layers of Stars." (1925).

Pearson, D. G., et al. "Hydrous mantle transition zone indicated by ringwoodite included within diamond." *Nature* 507.7491 (2014): 221-224.

Petigura, Erik A., Andrew W. Howard, and Geoffrey W. Marcy. "Prevalence of Earth-size planets orbiting Sun-like stars." *Proceedings of the National Academy of Sciences* 110.48 (2013): 19273-19278.

Phillips, Roger J., et al. "Impact craters and Venus resurfacing history." *Journal of Geophysical Research: Planets* 97.E10 (1992): 15923-15948.

Poppe, Torsten, Jürgen Blum, and Thomas Henning. "Analogous experiments on the stickiness of micron-sized preplanetary dust." *The Astrophysical Journal* 533.1 (2000): 454.

Pottasch, S. R. "A comparison of the chemical composition of the solar atmosphere with meteorites." *Annales d'Astrophysique*. Vol. 27. 1964.

Render, J., et al. "The cosmic molybdenum-neodymium isotope correlation and the building material of the Earth." *Geochem. Perspect. Lett.* 3 (2017): 170-178.

Ringwood, A. E. "A model for the upper mantle." *Journal of Geophysical Research* 67.2 (1962): 857-867.

Ringwood, A. E. "Genesis of chondritic meteorites." *Reviews of Geophysics* 4.2 (1966): 113-175.

Ringwood, Alfred Edward. *Composition and petrology of the earth's mantle [by] AE Ringwood*. 1975.

Ringwood, Alfred Edward. "Phase transformations in the mantle." *Earth and Planetary Science Letters* 5 (1968): 401-412.

Rubie, David C., et al. "Heterogeneous accretion, composition and core–mantle differentiation of the Earth." *Earth and Planetary Science Letters*301.1 (2011): 31-42.

Russell, Henry Norris. "The cosmical abundance of the elements." (1941): 647.

Russell, N., Cecilia H. Payne Gaposchkin, and D. H. Menzel. "The Classification of Stellar Spectra." *The Astrophysical Journal* 81 (1935): 107.

Safronov, Viktor Sergeevich. "Evolution of the Protoplanetary Cloud and Formation of the Earth and Planets." *Evolution of the protoplanetary cloud and formation of the earth and planets, by Safronov, VS. Translated from Russian. Jerusalem (Israel): Israel Program for Scientific Translations, Keter Publishing House, 212 p.* 1 (1972).

Savage, M. K., K. M. Fischer, and C. E. Hall. "Strain modelling, seismic anisotropy and coupling at strike-slip boundaries: applications in New Zealand and the San Andreas fault." *Geological Society, London, Special Publications* 227.1 (2004): 9-39.

Schuler, Simon C., and Jeremy R. King. "Stellar Nucleosynthesis in the Hyades Open Cluster." *The Astrophysical Journal* 701.1 (2009): 837.

Searle, Leonard, and Wallace LW Sargent. "Studies of the Peculiar a Stars. II. The Silicon-Abundance Anomaly." *The Astrophysical Journal* 139 (1964): 793.

Segura, Antígona, et al. "The effect of a strong stellar flare on the atmospheric chemistry of an Earth-like planet orbiting an M dwarf." *Astrobiology* 10.7 (2010): 751-771.

Shu, Frank H., Hsien Shang, and Typhoon Lee. "Toward an astrophysical theory of chondrites." *Science* 271.5255 (1996): 1545.

Smith, dgw. "Wadsleyite, natural F-(Mg, Fe). SiOn from the Peace River Meteorite." *Canadian Mineralogist* 21 (1983): 29-35.

Smith, J. V. "Possible controls on the bulk composition of the earth-Implications for the origin of the earth and moon." *Lunar and Planetary Science Conference Proceedings*. Vol. 8. 1977.

Smrekar, S. E., and A. Davaille. "Sublimating Paradigms on Venus: Volatiles, Episodic Tectonics, and Subduction." *AGU Fall Meeting Abstracts*. 2016.

Solanki, Sami K. "Structure of the solar photosphere." *Space science reviews*85.1-2 (1998): 175-186.

Sotin, Ch, O. Grasset, and A. Mocquet. "Mass–radius curve for extrasolar Earth-like planets and ocean planets." *Icarus* 191.1 (2007): 337-351.

Stevenson, David J., Tilman Spohn, and Gerald Schubert. "Magnetism and thermal evolution of the terrestrial planets." *Icarus* 54.3 (1983): 466-489.

Stixrude, Lars, and Carolina Lithgow-Bertelloni. "Thermodynamics of mantle minerals-II. Phase equilibria." *Geophysical Journal International* 184.3 (2011): 1180-1213.

Swedenborg, Emanuel. (Principia) Latin: Opera Philosophica et Mineralia (English: Philosophical and Mineralogical Works), (Principia, Volume 1) (1734).

Taylor, G. Jeffrey. "The bulk composition of Mars." *Chemie Der Erde-Geochemistry* 73.4 (2013): 401-420.

J.B. Thompson Jr 1982. Reaction Space: An algebraic and geometric approach. *Reviews in Mineralogy* (volume 10.) Characterization of Metamorphism Through Mineral Equilibria.

Tonks, W. Brian, and H. Jay Melosh. "Magma ocean formation due to giant impacts." *Journal of Geophysical Research: Planets* 98.E3 (1993): 5319-5333.

Unsöld, A., and O. Struve. "On the Number of Balmer Lines in Early-Type Stars." *The Astrophysical Journal* 91 (1940): 365.

Unterborn, Cayman T., Evan E. Dismukes, and Wendy R. Panero. "Scaling the Earth: A sensitivity analysis of terrestrial exoplanetary interior models." *The Astrophysical Journal* 819.1 (2016): 32.

Unterborn, Cayman T., et al. "Stellar Chemical Clues As To The Rarity of Exoplanetary Tectonics." *arXiv preprint arXiv:1706.10282* (2017).

Vagnozzi, Sunny. "New solar metallicity measurements." *arXiv preprint arXiv:1703.10834* (2017).

Valencia, Diana, and Richard J. O'Connell. "Convection scaling and subduction on Earth and super-Earths." *Earth and Planetary Science Letters* 286.3-4 (2009): 492-502.

Vanderburg, Andrew, et al. "Planetary candidates from the first year of the K2 mission." *The Astrophysical Journal Supplement Series* 222.1 (2016): 14.

Von Weizsäcker, C. F. "Über Elementumwandlungen in Innern der Sterne. II." *Physikalische Zeitschrift* 39 (1938): 633.

Wang, Lu, et al. "Partial melting of deeply subducted eclogite from the Sulu orogen in China." *Nature communications* 5 (2014).

Wade, J., and B. J. Wood. "Core formation and the oxidation state of the Earth." *Earth and Planetary Science Letters* 236.1 (2005): 78-95.

Walsh, Allan. "The application of atomic absorption spectra to chemical analysis." *Spectrochimica Acta* 7 (1955): 108-117.

Warren, Paul H. "The magma ocean concept and lunar evolution." *Annual Review of Earth and Planetary Sciences* 13.1 (1985): 201-240.

Watt, J. Peter, and Thomas J. Ahrens. "The role of iron partitioning in mantle composition, evolution, and scale of convection." *Journal of Geophysical Research: Solid Earth* 87.B7 (1982): 5631-5644.

Weller, Matthew B., and Adrian Lenardic. "On the evolution of terrestrial planets: Bi-stability, stochastic effects, and the non-uniqueness of tectonic states." *Geoscience Frontiers* 9.1 (2018): 91-102.

Wood, Bernard J., Ekaterina S. Kiseeva, and Andrew K. Matzen. "Garnet in the Earth's Mantle." *Elements* 9.6 (2013): 421-426.

Wood, John A. "The solar system." *The Prentice-Hall Foundations of Earth Science Series, Englewood Cliffs: Prentice-Hall, 1979* 1 (1979).

Woodhouse, John H., and Adam M. Dziewonski. "Mapping the upper mantle: Three-dimensional modeling of Earth structure by inversion of seismic waveforms." *Journal of Geophysical Research: Solid Earth* 89.B7 (1984): 5953-5986.

Woolfson, Michael. "The origin and evolution of the solar system." *Astronomy & Geophysics* 41.1 (2000): 1-12.

Yamamoto, Junji, and Hiroyuki Kagi. "Application of densimetry using micro-Raman spectroscopy for CO2 fluid inclusions: a probe for elastic strengths of mantle minerals." *European Journal of Mineralogy* 20.4 (2008): 529-535.

Yanick, Richard, Ondřej Šrámek, and Fabien Dubuffet. "A multi-phase model of runaway core–mantle segregation in planetary embryos." *Earth and Planetary Science Letters* 284.1 (2009): 144-150.

Yoshino, Takashi, et al. "Dry mantle transition zone inferred from the conductivity of wadsleyite and ringwoodite." *Nature* 451.7176 (2008): 326-329.

Yu, Yonggang G., et al. "Thermodynamic properties of MgSiO3 majorite and phase transitions near 660 km depth in MgSiO3 and Mg2SiO4: A first principles study." *Journal of Geophysical Research: Solid Earth* 116.B2 (2011).

Zeng, Li, Dimitar D. Sasselov, and Stein B. Jacobsen. "Mass–radius relation for rocky planets based on PREM." *The Astrophysical Journal* 819.2 (2016): 127.